Y-Box Binding Protein-1 Down-Regulates Expression of Carbamoyl Phosphate Synthetase-I by Suppressing CCAAT Enhancer-Binding Protein-Alpha Function in Mice

YEN-RONG CHEN,* KEISUKE SEKINE,‡ KOJI NAKAMURA,§ HIROYUKI YANAI,§ MINORU TANAKA,* and ATSUSHI MIYAJIMA*

*Institute of Molecular and Cellular Biosciences, The University of Tokyo; ‡Meikai University School of Dentistry, Sakado; and §LivTech, Kawasaki, Japan

BACKGROUND & AIMS: Carbamoyl phosphate synthetase-I (CPS1) is a key enzyme in the urea cycle and patients with defects in the function or expression of CPS1 suffer from hyperammonemia. CPS1 is expressed in the liver at neonatal and adult stages in a CCAAT enhancer-binding protein-alpha (C/EBPα)-dependent manner. Despite expression of C/EBPα, CPS1 is not expressed in fetal liver, indicating an additional factor is involved in the regulation of CPS1 expression. The aim of this study was to elucidate the mechanism of CPS1 expression. **METHODS:** Microarray was performed to find Y-box binding protein-1 (YB-1) that was expressed in mouse fetal liver. The role of YB-1 in CPS1 expression was investigated by overexpression of YB-1 in mouse fetal liver culture and luciferase reporter assays using the CPS1 promoter. Chromatin immunoprecipitation assay was used to examine recruitment of YB-1 to the CPS1 promoter in vivo. **RESULTS:** Expression of YB-1 and CPS1 was inversely correlated in vivo, and YB-1 inhibited CPS1 expression and ammonia clearance in fetal liver culture. Although YB-1 was not expressed in adult liver, acute liver injury up-regulated YB-1 and down-regulated CPS1, accompanying an increase of the serum ammonia level. YB-1 inhibited C/EBPα-induced transcription from the CPS1 promoter via the Y-box near the C/EBPα-binding site. Chromatin immunoprecipitation assays demonstrated that YB-1 was recruited to the CPS1 promoter in fetal and injured adult liver, but not in normal adult liver. **CONCLUSIONS: YB-1 is a key regulator of ammonia detoxification by negatively regulating CPS1 expression via suppression of C/EBPα function.**

The liver functions as a major hematopoietic organ in the fetus and acquires various metabolic functions during perinatal and neonatal stages. Among numerous liver functions in adult, ammonia detoxification is essential for life and excess ammonia in the body can be fatal. The nervous system is particularly sensitive to excessive ammonia and impaired clearance of ammonia is a major cause of hepatic encephalopathy.[1,2] A majority of the excess ammonia in mammals is converted into urea via the urea cycle, also known as the ornithine cycle, in the liver. Urea is then excreted by the kidneys. Glutamine synthetase (GS) also contributes to the metabolism of ammonia by converting it to glutamine. The urea cycle includes 5 major enzymes: carbamoylphosphate synthetase-I (CPS1), ornithine transcarbamylase, argininosuccinate synthetase, argininosuccinate lyase, and arginase. CPS1 catalyzes the first and rate-limiting step of the urea cycle, the formation of carbamoyl phosphate from ammonia and bicarbonate. It has been well established that defects in the function or expression of CPS1 causes hyperammonemia, which can result in brain damage and even death.[2,3] CPS1-deficient mice die soon after birth with overwhelming hyperammonemia.[4] These observations indicate that regulation of CPS1 expression is crucial for ammonia detoxification.

Analysis of the CPS1 promoter using hepatoma cell lines revealed that there are several *cis* regulatory elements required for the maximum promoter activity: a GAGA box at around −55 bp, a CCAAT enhancer-binding protein-alpha (C/EBPα) protein binding sequence at around −110 bp, and a glucocorticoid-response element (GRE) at around −95 bp. In addition to the promoter region, there is an enhancer region at −6.3kb from the transcription starting site, which contains C/EBP protein binding sites, GRE, FoxA/HNF3 binding sites, and cyclic AMP-response elements (see Figure 3*A*).[5–7] The −6.3 kb-distal enhancer region was suggested to interact with the proximal promoter by a glucocorticoid receptor (GR) homodimer that binds both regions via GREs and to induce CPS1 transcription.[8] C/EBPα-deficient mice lack CPS1 expression and exhibit hyperammonemia,[9] indicating that C/EBPα is essential for CPS1 expression. During liver development, CPS1 is expressed at the neonatal

Abbreviations used in this paper: CPS1, carbamoyl phosphate synthetase-I; C/EBPα, CCAAT enhancer-binding protein-alpha; CCl_4, carbon tetrachloride; ChIP, chromatin immunoprecipitation; Dlk, Delta-like protein; EGFP, enhanced green fluorescent protein; G6Pase, glucose-6-phosphatase; GS, glutamine synthetase; GR, glucocorticoid receptor; GRE, glucocorticoid-response element; GS, glutamine synthetase; HCC, human hepatocellular carcinoma; MDR1, multidrug resistant 1; PEPCK, phosphoenolpyruvate carboxykinase; TAT, tyrosine aminotransferase; YB-1, Y-box binding protein-1.

0016-5085/09/$36.00
doi:10.1053/j.gastro.2009.02.064

stage; C/EBPα as well as other positive regulators—GR, HNF3—are expressed in the fetal liver. Thus, an additional factor is suggested to be involved in the regulation of CPS1 expression.

By microarray analysis of mouse hepatocytes at different developmental stages, we found that Y-box binding protein-1 (YB-1) was highly expressed in fetal liver and was down-regulated along with development. Because YB-1 expression was inversely correlated with CPS1 expression during development, in this study, we examined the role of YB-1 in CPS1 expression. YB-1 is a multifunctional DNA/RNA binding protein belonging to the cold shock domain family, which is widely distributed from bacteria to mammals.[10] YB-1 is a transcription factor recognizing the *cis*-regulatory element, Y-box, defined as a reverse CCAAT box or ATTGG.[11] YB-1 is also an RNA-binding protein involved in the splicing, transport, and translation of mRNA and is implicated in DNA repair.[12,13] Y-box is present in the promoter of many genes such as the multidrug-resistant 1 (*MDR1*), major histocompatibility complex class II, epidermal growth factor receptor, DNA polymerase, thymidine kinase, and topoisomerase II genes. YB-1 promotes proliferation of tumor cells, such as breast, ovarian, lung, and prostate cancers, and up-regulates the expression of *MDR1*.[14] YB-1 is also considered as a tumor marker of human hepatocellular carcinoma (HCC).[15] In an inflamed liver, it suppresses the formation of collagen and modulates fibrosis.[16] The liver in YB-1–deficient mice is small and the mutant mice die soon after birth.[17] These results suggest that YB-1 plays an important role in the liver. However, its function during liver development and in adults remains elusive. Because YB-1 expression was inversely correlated with CPS1 expression, we investigated role of YB-1 in CPS1 expression and revealed that YB-1 represses CPS1 expression and plays a critical role in the metabolism of ammonia in developing hepatocytes as well as acute hyperammonemia in mouse adult liver.

Materials and Methods

Mice, Cells, and Cell Culture

C57BL/6 mice (Nihon SLC, Hamamatsu, Japan) were used for all the experiments under Guidelines of the University of Tokyo for Animal Care. 293T and HepG2 cells and BOSC23 cells were cultured in Dulbecco's modified Eagle's medium (Invitrogen, Carlsbad, CA) containing 10% fetal calf serum and 50 μg/ml of gentamycin. Mouse fetal liver cells were cultured as reported.[18] Hepatic progenitor cells proliferating on laminin cells were cultured as reported.[19]

Microarray Analysis

Mouse hepatoblasts were isolated from E12.5 and E17.5 fetal liver using anti-mouse Delta-like protein (Dlk) monoclonal antibody according to a previous report[19] and dissolved in Trizol reagent. The cDNA samples synthesized from total RNA were used for a microarray analysis with the mouse GEM2 microarray. Microarray data can be assessed by the following link: http://www.ncbi.nlm.nih.gov/geo/query/acc.cgi?token=fdilvegmiwowqvy&acc=GSE13363.

Luciferase Reporter Assay

Transfection was performed using Lipofectamine plus reagent, according to the manufacturer's instructions (Invitrogen). The luciferase assay was performed according to the manufacturer's instructions (Promega, Madison, WI). Each experiment was performed in triplicate. All experiments using 293T and HepG2 cells were performed with at least three different cell preparations.

Plasmids and Antibodies

Mouse C/EBPα cDNA was cloned by polymerase chain reaction into a pcDNA3 vector (Invitrogen) based on the reported sequence.[20,21] YB-1 and GR cDNAs were inserted into pcDNA3 (Invitrogen). A retroviral vector for YB-1 expression was constructed using the plasmid pMXIG. The proximal region (−600 to +10) and distal-proximal region (−6.3 kb element; 451 bps)[6] were inserted into pGL4-luc vector (Promega). The distal element (−6.3 kb element; 451 bps) was connected to the proximal region as shown in Figure 3*C* and cloned into pGL4-luc (Figure 3*B*, *C*). Antibodies used in this study were: anti-C/EBPα (14AA; Santa Cruz Biotech, Santa Cruz, CS), anti-YB1 (ab12148; Abcam, Cambridge, MA), anti-CPS1 (E-20, Santa Cruz Biotech), and anti-actin (I-19, Santa Cruz Biotech).

Northern and Western Blotting

As described previously,[21] Northern and Western blottings were performed. Total RNA from E14.5, E17.5, neonatal, and adult mouse livers (4 and 8 weeks old), and also from cultured cells was extracted by using Trizol solution (Invitrogen) and then analyzed by Northern blotting. Livers from E14.5, E17.5, neonatal, and adult mice (4 and 8 weeks old) were homogenized and lysed. Protein samples were subjected to sodium dodecyl sulfate-PAGE, and immunoblotted using antibodies against YB-1, CPS1, or C/EBPα.

Retroviral Infection

Retroviral vectors were transfected into BOSC23 cells by lipofection and the viral particles were harvested after 2 days. The particles were collected by centrifugation at 6000 *g* for 16 hours at 4°C and pellets were resuspended in fetal hepatocyte culture medium. Fetal hepatocytes grown in 6-well plates for 2 days after plating were incubated with the viral suspension. After 2 days, the culture medium was changed to a virus-free fetal hepatocyte culture medium.

Chromatin Immunoprecipitation Assay

The chromatin immunoprecipitation (ChIP) assay was performed with a kit (Upstate), and also described previously.[21] Polymerase chain reaction was performed with the following primers:

CPS1: sense (-300), 5′-TGCATTATTAGCAAGGTACT-GCCC-3′; anti-sense (-50), 5′-TTCCTTAGCCCCTC-CTCCCAAGCTG-3′.

β-Actin: sense (-75), 5′-GTTCCGAAAGTTGCCTTTT-ATG-3′; anti-sense (+252), 5′-ATGTGGCTGCAAAG-AGTCTACA-3′.

Mouse Liver Injury by CCl_4 and Acetaminophen

Liver injury was induced by an IP injection at a dose of 500 mg/kg body weight acetaminophen dissolved in phosphate-buffered saline (Sigma, St Louis, MO) or a 20% (v/v) solution of CCl_4 (Wako Pure Chemicals, Osaka, Japan) in corn oil at a dose of 7 μL/g body weight.[22]

Ammonia and Urea Levels

To examine the cellular activity to clear ammonia and produce urea, fetal hepatocytes were loaded with 2 mmol/L NH_4Cl at day 7 after plating and further incubated for 0–72 hours.[23] Concentrations of ammonia in culture media were measured by the modified indophenol method using a commercial kit (Ammonia-Test Wako; Wako Pure Chemical Industries). Concentrations of urea were measured by a urea assay kit (Quantichom Urea assay kit; BioAssay systems, Hayward, CA). The blood of CCl_4-treated mice was drawn and analyzed with the same kit.

Results

Gene Expression Profiles of Mouse Hepatoblasts/Immature Hepatocytes During Development

Mouse hepatoblasts emerging at E8.5 from the foregut endoderm proliferate vigorously and differentiate to hepatocytes and biliary epithelial cells.[24] To find genes important for hepatocyte differentiation during development, we compared gene expression profiles of mouse hepatoblasts/immature hepatocytes at E12.5 and E17.5. Because Dlk, also known as Pref-1, is expressed in hepatoblasts/immature hepatocytes,[19] we performed a microarray analysis of the Dlk^+ cells isolated from livers at E12.5 and E17.5. Consistent with the high proliferative potential of hepatoblasts in the early stages, cyclins D1, D2, and E were highly expressed in E12.5 hepatoblasts (Table 1). Among the top 30 genes preferentially expressed in E12.5 hepatoblasts, there were several transcription factors such as HMGA1, CITED, FoxM1, GATA6, and YB-1. In this study, we have focused on YB-1.

Northern blot analysis revealed that YB-1 was highly expressed in E14.5 liver, but its expression was significantly down-regulated at E17.5 and was absent in adult liver. Consistent with a report that cyclin A expression was regulated by YB-1,[25] cyclin A was also highly ex-

Table 1. Genes Highly Expressed in E12.5 Hepatoblasts

No.	Gene name	Accession no.	No.	Gene name	Accession no.
1	Midkine	AI325764	19	Y box protein 1	AA450785
2	High mobility group AT-hook 1	AA067083	20	Serum response factor	AA415341
3	Cbp/p300-interacting transactivator with Glu/Asp-rich carboxy-terminal domain 1	AA709508	21	Teratocarcinoma expressed, serine rich	AA116831
4	Cyclin D1	AA117547	22	Small inducible cytokine B subfamily (Cys-X-Cys), member 10	AI158236
5	Cyclin D2	AA879568			
6	Cyclin E	AA437868	23	Cyclin F	AI326604
7	Dickkopf homolog 3	AA073904	24	Stromal cell derived factor 1	AA066069
8	Nik related kinase	AI225895	25	Epidermal growth factor-containing fibulin-like extracellular matrix protein 2	AW210333
9	TEA domain family member 2	AA617316			
10	Forkhead box M1	AW519587			
11	Tcra enhancer-binding factor interacting protein 1	AA437646	26	Ras-GTPase-activating protein (GAP) SH3-domain-binding protein 2	AA617613
12	Transmembrane 4 superfamily member 6	AA437557			
13	Cysteine rich protein 61	AA466852	27	Transforming, acidic coiled-coil containing protein 3	AA190123
14	Integral membrane protein 2	AA387218	28	EphA4	AI325333
15	Cyclin-dependent kinase 4	AI892404	29	Enhancer of zeste homolog 2	AA445767
16	GATA-6	AA536899	30	NPC derived proline rich protein 1	AA791966
17	Pleiotrophin	AI047160			
18	CDk2-associated protein 1	AA638778			

Dlk+ hepatoblasts were isolated from E12.5 and E17.5 fetal liver using AutoMACS. Gene expression analysis was performed using a Mouse GEM2 microarray.

pressed in E14.5 liver, but was diminished at E17.5. In contrast, C/EBPα was constitutively expressed from E14.5 to adulthood, and the expression of CPS1 and GS was up-regulated at the neonatal stage (Figure 1*A*). Western blotting also confirmed that YB-1 protein was present in E14.5 and E17.5 liver, but not in neonatal liver, and 2 C/EBPα isoforms were expressed constitutively (Figure 1*B*). CPS1 was expressed from neonatal liver (Figure 1*B*). Although YB-1 mRNA expression was significantly down-regulated at E17.5, YB-1 protein was still detected at this stage, suggesting that YB-1 protein is stable in mouse hepatoblasts.

YB-1 Inhibits Expression of CPS1

To reveal the role of YB-1 in the maturation of hepatocytes, we took advantage of a primary culture system, in which fetal hepatocytes can be induced to differentiate by oncostatin M.[18] In this culture system, many metabolic enzymes such as CPS1, tyrosine aminotransferase (TAT), and glucose-6-phosphatase (G6Pase) were undetectable for the first 3 days and were detected at day 7 after plating (Figure 1*C* and *D*). By contrast, YB-1 mRNA and protein were present for the first 3 days and diminished at 7 days after plating, whereas C/EBPα was constitutively expressed during the culture period (Figure

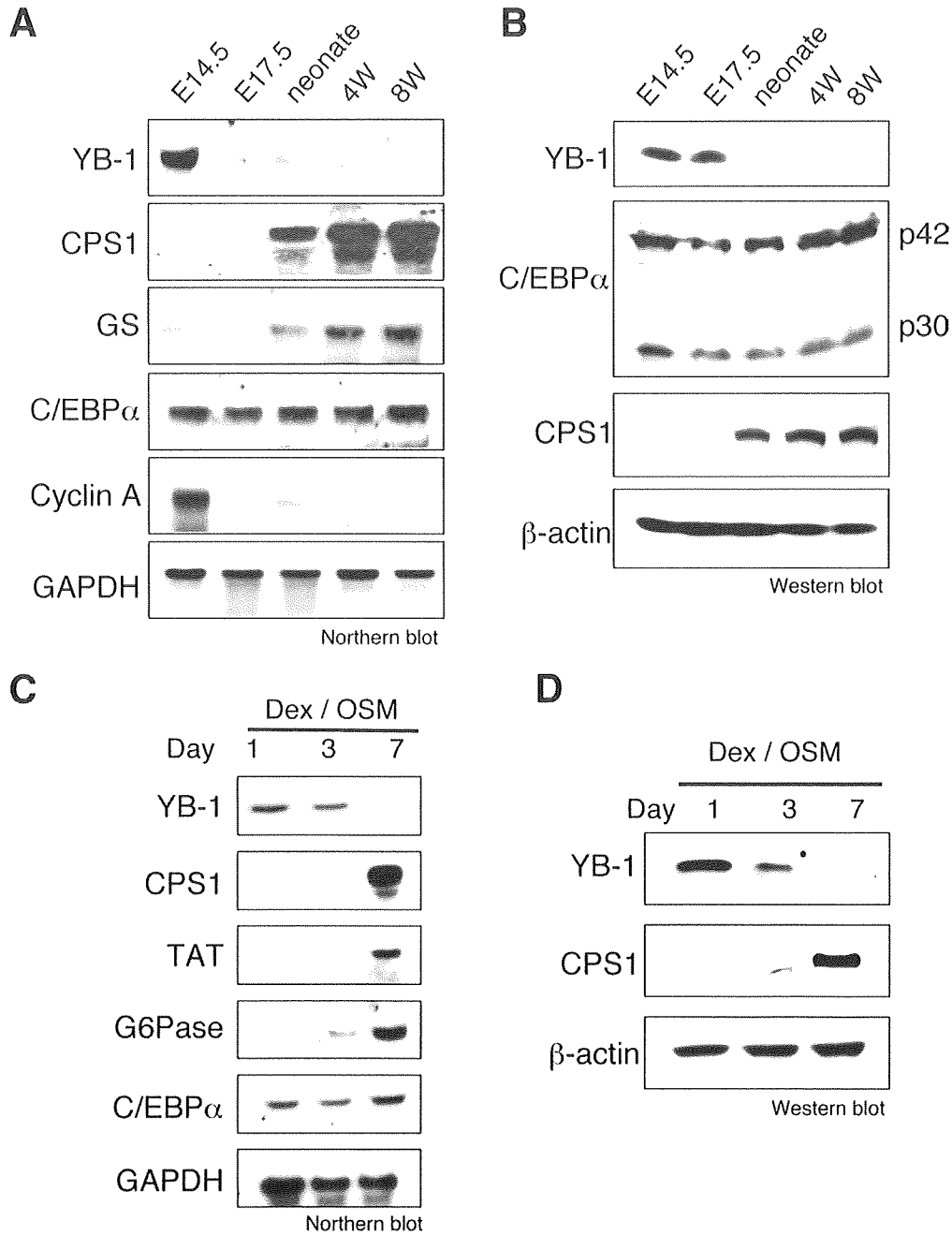

Figure 1. Expression of YB-1 during mouse fetal liver development. (*A*) Expression of various mRNA as shown during liver development by Northern blot analysis. RNA was prepared from mouse liver tissues at E14.5, E17.5, the neonatal period, and 4- and 8-week-old mice. (*B*) Protein levels of YB-1, C/EBPα isoforms (p42 and p30), CPS1, and β-actin during liver development. The protein levels in whole cell extracts from the liver at different stages were examined by Western blot analysis. (*C*) Expression of mRNA in fetal hepatic cultures. E14.5 fetal liver cells were cultured and RNA was prepared for Northern blot. (*D*) Protein levels of YB-1, CPS1, and β-actin in fetal hepatic cultures. Mouse E14.5 fetal liver cells were cultured and protein was prepared for Western blot analysis.

1C and *D*). The results are consistent with YB-1 expression during liver development in vivo (Figure 1*A*); that is, YB-1 expression is strong in immature liver, but is weak in adult liver.

To investigate the role of YB-1 protein in the maturation of hepatocytes, we overexpressed YB-1 in cultured mouse fetal liver cells using a retroviral vector encoding both YB-1 and enhanced green fluorescent protein (EGFP) proteins. The efficiency of the infection was estimated to be about 65% based on an analysis of EGFP expression by flow cytometry. In the control culture, fetal hepatocytes differentiated, as shown by the morphology of mature hepatocytes and expression of liver enzymes such as TAT, G6Pase, and CPS1. In the cultures infected with the YB-1-encoded retrovirus, the expression of a YB-1 target gene, cyclin A, was up-regulated (Figure 2*A*). Although the morphology of the hepatocytes (data not shown) and expression of TAT and G6Pase were similar to those in the control culture (Figure 2*A*), CPS1 expression was severely inhibited. In contrast with CPS1, a key enzyme for the urea cycle, expression of GS, which also contributes to ammonia clearance to a limited extent, was not affected by YB-1. In addition, YB-1 did not change the gene expression of other enzymes in the urea cycle such as ornithine transcarbamylase, argininosuccinate synthetase, argininosuccinate lyase, or arginase (data not shown). Besides, knockdown of YB-1 expression by small interfering RNA up-regulated CPS1 expression in a hepatoblast cell line (Supplementary Figure 1). These results indicated that expression of CPS1 and YB-1 was inversely correlated in vitro as well as in vivo (Figure 1), suggesting that YB-1 is a negative regulator of CPS1 expression. By contrast, the expression of cyclin A was up-regulated by YB-1 (Figure 2*A*).

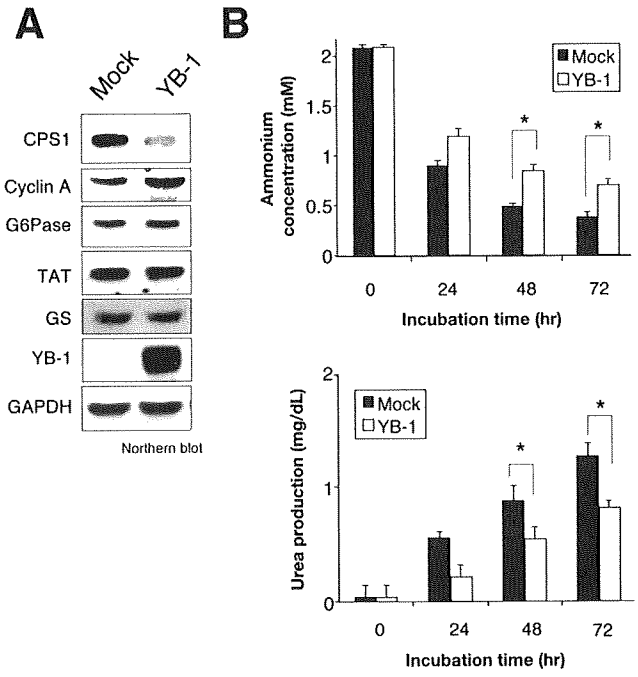

Figure 2. The effect of YB-1 on CPS1 expression and ammonia clearance in mouse fetal liver cells. (*A*) YB-1 was expressed using a retroviral system in the fetal liver culture. The levels of mRNA of CPS1, cyclin A, G6Pase, TAT, GS, YB-1, and GAPDH at 7 days after the infection were examined by Northern blot analysis. (*B*) The ammonia and urea production levels in the culture medium of fetal liver culture. The medium was changed to the one containing ammonia 3 days after the retroviral infection and the ammonia and urea levels were determined at different time points as indicated. Because serum in the culture medium contained urea, the data shown are urea produced during culture, that is, the serum urea level was subtracted from the amount of urea measured in the cultured media. The ability of the cells overexpressing YB-1 to metabolize ammonia was less than that of control cells. Error bars represent + standard deviations. $^*P < .05$.

Inverse Correlation Between YB-1 Expression and Ammonia Clearance

CPS1 is a key enzyme involved in ammonia detoxification in mammals. To investigate whether YB-1 regulates ammonia levels, we evaluated the ability of hepatocytes to metabolize ammonia in the primary culture of E14.5 liver cells infected with a retrovirus encoding YB-1. After 7 days of culture, the medium was replaced with ammonia-containing medium and the ammonia concentration was measured. Ammonia-containing medium did not affect viability, gene expression, or morphology of the cultured cells (Supplementary Figure 2). The ammonia levels were higher in the culture medium infected with YB-1-encoded virus than the control culture (Figure 2*B*), consistent with the CPS1 expression. In contrast with ammonia levels, urea production in the culture infected with virus carrying YB-1 cDNA was lower than the control culture (Figure 2*B*). These results indicate that CPS1 expression modulated by YB-1 is critical for ammonia clearance and urea production.

YB-1 Inhibits C/EBPα-Mediated CPS1 Transcription

To further investigate the role of YB-1 in CPS1 expression, a luciferase reporter assay was used to determine whether or not YB-1 affected transcription from the mouse CPS1 promoter. Previous studies on the CPS1 promoter identified 2 regions important for CPS1 expression, namely, the distal −6.3-kb enhancer and the proximal promoter (Figure 3*A*).[6,26] First, we cloned the promoter region of the CPS1 gene covering 600 nucleotides from the transcription starting site, and inserted it into the pGL4 luciferase reporter vector, pGL4-CPS1 (proximal)-Luc (Figure 3*B*, *upper scheme*). Because CPS1 expression requires C/EBPα and there is a C/EBPα recognition site in the promoter fragment,[26] we examined the effect of C/EBPα on CPS1 transcription. Although luciferase was not expressed by transfection of the reporter construct with the CPS1 promoter alone, co-transfection of the C/EBPα expression vector dramatically induced the expression of luciferase from the CPS1 promoter in 293T or HepG2 cells (Figure 3*B*; Supplementary

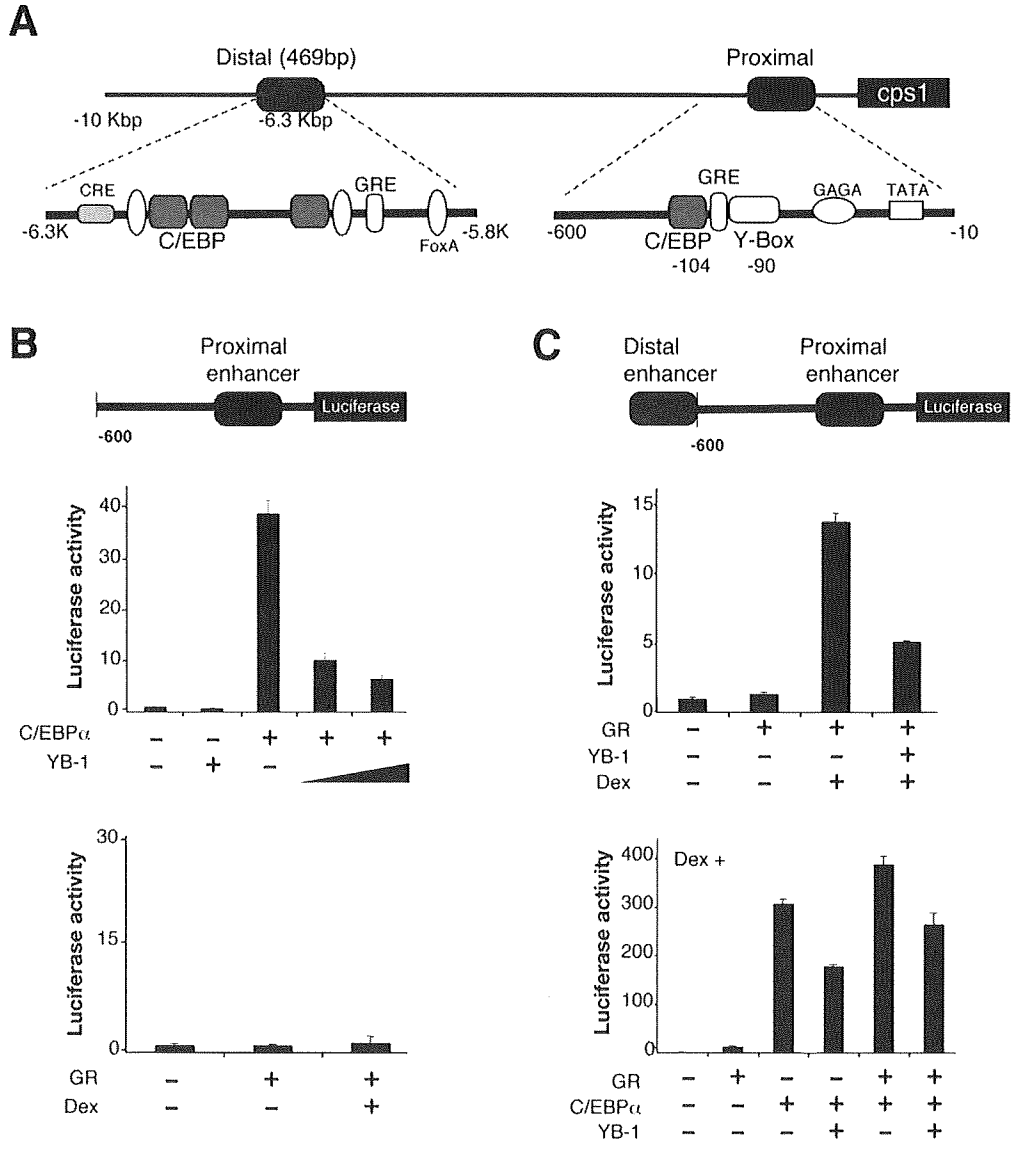

Figure 3. Suppression of transcription from the CPS1 promoter by YB-1. (*A*) The distal enhancer and proximal enhancer of the CPS1 gene promoter. (*B*) Structure of pGL4-CPS1 (proximal)-Luc vector. (*C*) Structure of pGL4-CPS1 (distal–proximal)-Luc vector. 293T cells were transfected with the CPS1 promoter-Luc vectors together with the expression vectors for C/EBPα, GR, and YB-1 as indicated. Cells were harvested for luciferase assays 48 hours after transfection. Data shown are normalized by *Renilla* luciferase activity and are mean values + standard deviations. A representative experiment performed in triplicate is shown.

Figure 3*A*). We then co-expressed YB-1 and found that C/EBPα-induced expression of luciferase was severely inhibited by YB-1 in a dose-dependent manner (Figure 3*B*; Supplementary Figure 3*A*).

It was reported that the CPS1 promoter was activated by the distal −6.3-kb enhancer (distal). The enhancer was suggested to interact with the promoter by a GR–GR homodimer that binds the GRE sites in both regions (Figure 3*A*).[8] To investigate whether YB-1 also affects the −6.3-kb (distal) enhancer, we constructed pGL4-CPS1 (distal–proximal)-Luc, which contained both distal and proximal regions (Figure 3*C*).[8] GR is an essential factor for CPS1 expression and it, in fact, induced the transcription form pGL4-CPS1 (distal–proximal)-Luc in the presence of Dex. However, GR failed to do so from pGL4-CPS1 (proximal)-Luc (Figure 3*B*). C/EBPα induced transcription from pGL4-CPS1 (distal–proximal)-Luc stronger than GR (Figure 3*C*) and co-expression of GR and C/EBPα synergistically enhanced the transcription. Furthermore, YB-1 suppressed the transcription by either GR or C/EBPα alone and also by co-expression of GR and C/EBPα (Figure 3*C*; Supplementary Figure 3*A*). These results confirmed the previous results that the distal and proximal regions cooperatively induced CPS1 expression and indicated that YB-1 is a negative regulator of CPS1 expression.

YB-1 is known to bind the Y-box sequence, namely, inverted CCAAT, to regulate gene expression.[11] We found one inverted CCAAT sequence, ATTGG, at −90 in the CPS1 promoter (Figure 4*A*), which was only 10 nucleotides from the C/EBPα recognition site, GTTGCAATTTGTAT (Figure 4*A*).[26] Therefore, we considered the possibility that YB-1 binds to this site and inhibits the transcriptional activation of CPS1 by C/EBPα. We examined whether this Y-box is responsible for the suppression of C/EBPα-induced CPS1 transcription by mutating

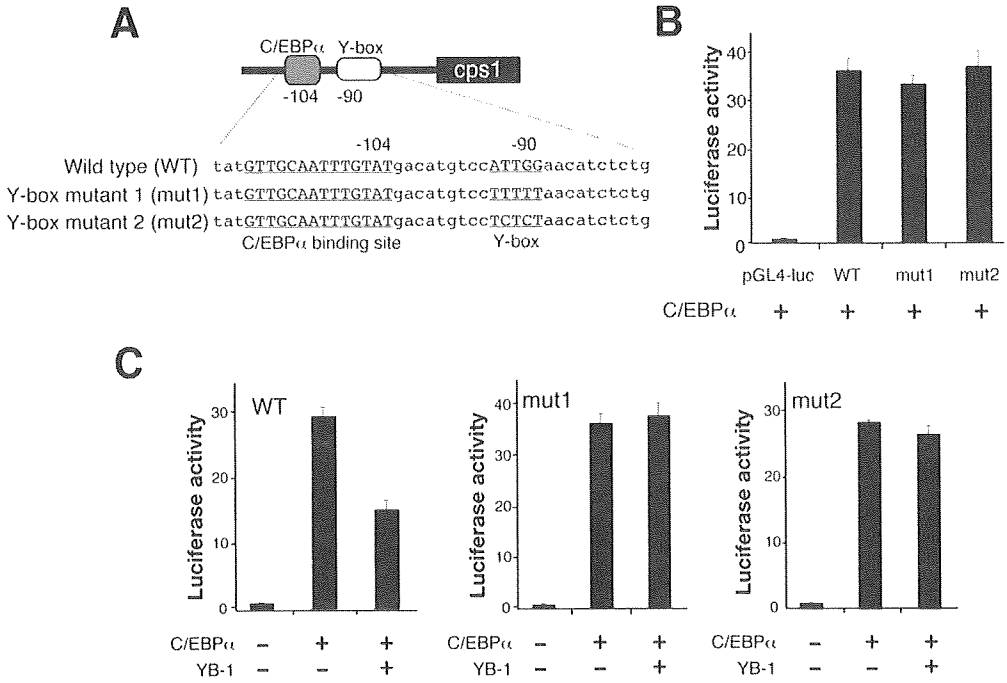

Figure 4. Suppression of transcription from the CPS1 promoter via Y-box site. (*A*) Nucleotide sequence of the promoter region of the CPS1 gene. There is an inverted CCAAT sequence at position −90 from the transcription start site of the CPS1 promoter and the C/EBPα binding site is between −104 and −117. The Y-box was mutated to TTTTT (Y-box mutant 1) and TCTCT (Y-box mutant 2). (*B*) C/EBPα and pGL4-CPS1 (proximal)-Luc plasmids were co-transfected into 293T cells with either CPS1 (proximal)-Luc (WT), Y-box mutant 1-Luc (mut1), or Y-box mutant 2-Luc (mut2) and luciferase activity was measured 48 hours later. (*C*) Wild-type, mut1, or mut2 was transfected with C/EBPα and YB-1 expression vectors as indicated and luciferase activity was measured 48 hours later. Data shown are normalized by *Renilla* luciferase activity and are mean values + standard deviations. A representative experiment performed in triplicate is shown.

the inverted CCAAT to TTTTT or TCTCT. These mutant promoters were still capable of expressing luciferase in a C/EBPα-dependent manner (Figure 4*B*); however, YB-1 failed to repress C/EBPα-dependent transcription from these 2 mutated promoters (Figure 4*D*). Roles of C/EBPα (−104) and YB-1 (−90) recognition sites in CPS1 gene enhancer were also tested by mutation analysis. Disruption of the C/EBPα site reduced the promoter activity, whereas the Y-box mutation rather enhanced the promoter activity in HepG2 cells (Supplementary Figure 3*B*). These results clearly indicated that the suppression of CPS1 promoter activity by YB-1 is mediated by the Y-box in the promoter.

YB-1 Is Recruited to the CPS1 Promoter in Fetal Liver

We examined if the YB-1 protein binds to the CPS1 promoter in E14.5 liver in vivo using ChIP assays. From E14.5 liver samples, anti-YB-1 antibody immunoprecipitated the target fragment, whereas it failed to do so in normal adult liver (Figure 5). By contrast, anti-C/EBPα antibody immunoprecipitated the target fragment from E14.5 as well as adult liver samples (Figure 5). These results indicate that YB-1 binds in vivo to the CPS1 promoter in fetal but not in normal adult liver.

YB-1 in Acute Hepatitis

Detoxification of ammonia is an essential liver function.[27] Because hyperammonemia is associated with liver injury, we examined the expression of CPS1 and YB-1 during acute liver injury induced by the administration of carbon tetrachloride (CCl_4). The serum ammonia level began to increase 24 hours after the administration of CCl_4, reached a peak at 48 hours, and then gradually declined to the basal level (Figure 6*B*). In contrast, the serum urea level was decreased at 48 hours after CCl_4 injection (Figure 6*B*). Northern blot analysis showed that the CPS1 mRNA level was transiently, but significantly, decreased in the liver at 24 hours after the CCl_4 injection. By contrast, the YB-1 and cyclin A mRNA levels were increased after the injection (Figure 6*A*, *left panel*). Protein levels of YB-1 and CPS1 were also inversely correlated (Figure 6*A*, *right panel*). The expression of C/EBPα was not changed significantly during this stage (Figure 6*A*). Moreover, ChIP assays showed that anti-YB-1 antibody precipitated the CPS1 promoter fragment in injured liver, but not in normal adult liver (Figure 6*C*). These results together indicate that YB-1 is recruited to the CPS1 promoter and regulates the metabolism of ammonia in injured liver.

As another model of liver injury, we employed acetaminophen-induced acute liver injury, in which CPS1

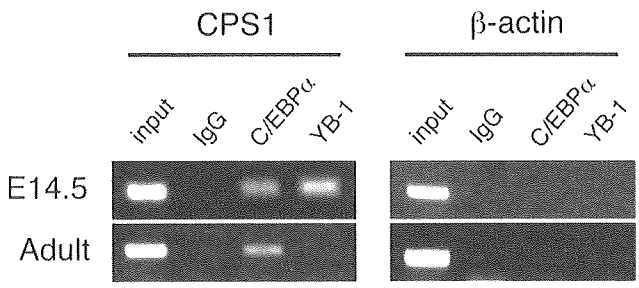

Figure 5. Recruitment of YB-1 in liver. Recruitment of C/EBPα and YB-1 to the target DNA demonstrated by chromatin immunoprecipitation assays. The association of C/EBPα and YB-1 with the endogenous CPS1 promoter (−300~−50) was detected by chromatin immunoprecipitation assays as described in Materials and Methods. The β-actin promoter fragment (−75~+252) failed to recruit C/EBPα and YB-1, indicating specific recruitment of these proteins to the CPS1 promoter.

activity is inhibited and concomitantly acute hyperammonemia is induced.[28] We found that the administration of acetaminophen up-regulated YB-1 expression and down-regulated CPS1 expression (Figure 6*D*). These results indicate that YB-1 expression is inversely correlated with CPS1 expression in adult mouse liver.

Discussion

YB-1 contains a cold shock domain that binds DNA and has been shown to regulate the expression of many genes, including the cyclin A, cyclin B, and *MDR1* genes.[25,29] YB-1 is highly expressed in fetal liver, injured liver (Figures 1*A* and *B*; and 6*A* and *D*), and also in HCC[15]; however, the role of YB-1 in the liver remained unclear. This study reveals a previously unrecognized important function of YB-1 for ammonia detoxification in mice. YB-1 expression was evident in the liver at E14.5, and declined along with liver maturation. Forced expression of YB-1 in fetal liver cells resulted in suppression of CPS1 expression. YB-1 bound to a Y-box in the CPS1 promoter, down-regulating the transcriptional activity induced by C/EBPα. Moreover, CCl_4-induced liver injury up-regulated YB-1 expression, accompanying the suppression of CPS1 and increase of serum ammonia and decrease of urea concentration. ChIP assays showed that YB-1 bound to the CPS1 promoter in fetal and CCl_4-injured livers, but not in normal adult liver in mice. Based on these results, we conclude that YB-1 is a negative regulator of CPS1 transcription.

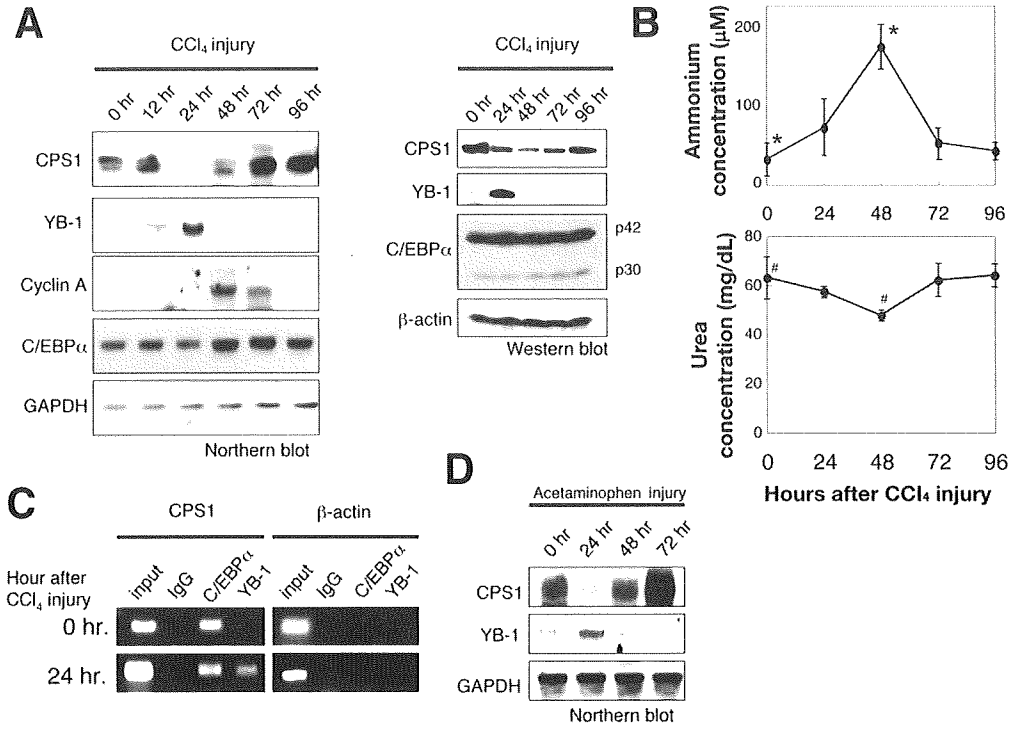

Figure 6. Expression and recruitment of YB-1 in CCl_4-impaired liver. (*A*) Expression of mRNA and protein in CCl_4-induced liver injury. CCl_4 was injected into the peritoneum of mice. RNA and protein were prepared from livers at different time points after the injection. The RNA and protein levels were determined by Northern and Western blot analyses. The level of YB-1 was increased at 24 hours after CCl_4 treatment, whereas the expression of CPS1 RNA decreased to an undetectable level at the same time point. The CPS1 protein level began to decrease at 24 hours after CCl_4 treatment. (*B*) The concentration of ammonia in serum was measured. The level began to rise from 24 hours after CCl_4 treatment, and reached a peak at 48 hours. The concentration of serum urea was measured. The level reached the lowest point at 48 hours. Error bars represent + standard deviations. $N = 4–6$. $^*P < .003$; $\#P < .002$. (*C*) Recruitment of C/EBPα and YB-1 to the target DNA demonstrated by chromatin immunoprecipitation assays. (*D*) Acetaminophen was injected into the peritoneum of mice and RNA was prepared from liver at different time points after the injection. RNA levels were determined by Northern blot analysis.

YB-1 Regulates CPS1 Expression

CPS1 is a key enzyme for the urea cycle and CPS1-deficient mice die with hyperammonemia.[4] A deficiency of CPS1 in humans also causes hyperammonemia that results in complications including developmental delay and mental retardation.[1] Thus, CPS1 is essential for ammonia detoxification and its expression requires C/EBPα.[9] CPS1 is not expressed in fetal liver and its expression requires C/EBPα in neonatal liver. Previous studies showed that CPS1 is regulated by several transcription factors, such as C/EBPα, HNF3, and GR.[6,26] The distal −6.3-kb enhancer and the proximal promoter of the *CPS1* gene are important for CPS1 expression. The GRE site is present in each region and has been considered to bridge the 2 regions via the GR–GR interaction.[8] Consistently with the previous studies we show that the −6.3-kb enhancer increases promoter activity induced by C/EBPα. This study has revealed that a Y-box is present only 10 nucleotides from the C/EBP-binding site in the CPS1 promoter and partially overlaps with the GRE (Figure 4*A*). Mutation analysis showed that the inhibition of C/EBPα-dependent luciferase expression by YB-1 was in fact mediated by this Y-box (Figure 4*B*; Supplementary Figure 3*B*). The Y-box we identified is consistent with the repressive element I in the CPS1 promoter, which was previously found in rat hepatoma cells.[30] YB-1 inhibits transcription from pGL4-CPS1 (proximal)-Luc as well as pGL4-CPS1 (distal-proximal)-Luc, indicating that YB-1 suppresses the cooperative transcription activation by C/EBPα and GR as well as C/EBPα alone. ChIP assays also indicated that YB-1 binds to the CPS1 promoter in both mouse fetal liver and regenerating liver damaged by administration of CCl_4, but not in normal adult liver (Figure 6C). These results strongly suggest that YB-1 physically interferes with the formation of transcription complex, which contains the transcription factors on the promoter and the distal enhancer.

The expression patterns of several metabolic genes, such as CPS1, phosphoenolpyruvate carboxykinase (PEPCK), TAT, and G6Pase during development, are very similar; in fact, their expression requires C/EBPα. However, each gene seems to be regulated by an additional mechanism. Expression of TAT and G6Pase also requires C/EBPα and putative Y-box sites are present in their 5′ untranslated regions; however, their expression was not affected by YB-1 (Figure 2*A*). Because their Y-boxes are far from the C/EBPα binding site in their promoters, the distance between the YB-1 and C/EBPα binding sites may be an important factor for YB-1 to inhibit C/EBPα function. In the case of PEPCK and G6Pase, their expression is also cooperatively regulated by C/EBPα and Foxo1, a target of insulin signaling.[21] Posttranslational modifications of the liver enriched transcription factors also affect the gene expression, such as SUMOylation of C/EBPα, is also considered to suppress TAT promoter transcriptional activity.[31] Thus, in addition to C/EBPα, several distinct mechanisms are involved in expression of metabolic genes during development.

Role of YB-1 in Liver Development and Injury

Immature hepatocytes proliferate vigorously in fetal liver and differentiate into mature hepatocytes around the time of birth. YB-1 is expressed in fetal liver and HCC, indicating a positive correlation between YB-1 expression and cell proliferation.[15,17,32] We showed that YB-1 and cyclin A were highly expressed in E14.5 mouse liver and disappeared with differentiation (Figure 1*A*). Although a weak signal for YB-1 mRNA was detected even after birth, YB-1 protein was not detected in normal adult liver by Western blotting (Figure 1*B*), suggesting there to be posttranscriptional or posttranslational regulation of YB-1 in the adult liver. The absence of YB-1 protein in normal liver is also supported by the ChIP assays. YB-1 was not expressed in adult liver, but was re-expressed in regenerating liver injured by the administration of CCl_4 or acetaminophen (Figure 6*A* and *D*).

The expression of YB-1 was shown to be up-regulated by c-Myc in cancer cells,[33] consistent with the co-expression of c-Myc and YB-1 in fetal hepatocytes and also HCC.[34] In CCl_4-injured liver, c-Myc expression is also up-regulated at an early phase.[35] Thus, YB-1 may be involved in the network of c-Myc-mediated signaling in liver. YB-1 was also shown to increase the expression of PTP1B, a protein tyrosine phosphatase, to regulate signaling pathways triggered by cytokines, growth factors, and hormones. The expression of antisense YB-1 in Rat1 cells enhanced gp130-mediated signaling,[36] suggesting YB-1 to play a role in the suppression of gp130-mediated signaling. Because gp130 is important for the expression

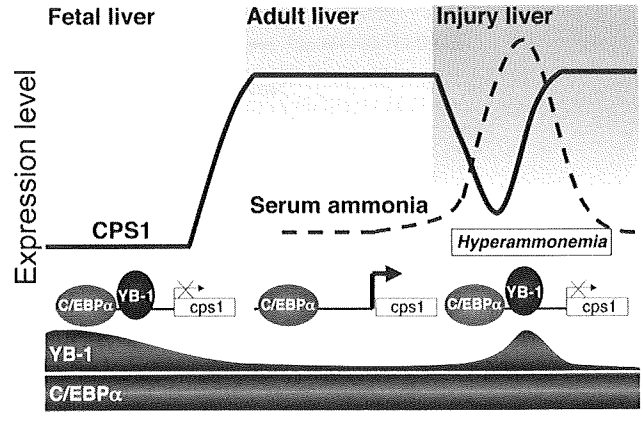

Figure 7. Role of YB-1 in CPS1 expression and ammonia detoxification. YB-1 is highly expressed in fetal liver and down-regulated along with differentiation, whereas C/EBPα is constitutively expressed. YB-1 is absent in normal adult liver, but is expressed in injured liver. In contrast, CPS1 is absent in fetal liver and expressed in normal liver. CPS1 expression is down-regulated in injured liver, accompanying hyperammonemia.

of liver functions,[18] the shutdown of YB-1 expression in the liver late in gestation may be necessary for gp130-mediated expression of various metabolic functions at the perinatal and postnatal stages. Taken together, these results strongly implicate YB-1 in the proliferation and also maturation of hepatocytes.

In conclusion, this study reveals that YB-1 regulates ammonia metabolism by modulating transcription of the CPS1 gene and solves a puzzle on CPS1 expression; although C/EBPα is essential for the CPS1 expression and is constitutively expressed in the liver throughout its development, CPS1 is not expressed in fetal liver (Figure 7).

Supplementary Data

Note: To access the supplementary material accompanying this article visit the online version of *Gastroenterology* at www.gastrojournal.org and at doi: 10.1053/j.gastro.2009.02.064.

References

1. Gropman AL, Batshaw ML. Cognitive outcome in urea cycle disorders. Mol Genet Metab 2004;81(Suppl 1):S58–62.
2. Takeoka M, Soman TB, Shih VE, et al. Carbamyl phosphate synthetase 1 deficiency: a destructive encephalopathy. Pediatr Neurol 2001;24:193–199.
3. Gelehrter TD, Snodgrass PJ. Lethal neonatal deficiency of carbamyl phosphate synthetase. N Engl J Med 1974;290:430–433.
4. Schofield JP, Cox TM, Caskey CT, et al. Mice deficient in the urea-cycle enzyme, carbamoyl phosphate synthetase I, die during the early neonatal period from hyperammonemia. Hepatology 1999;29:181–185.
5. Christoffels VM, Grange T, Kaestner KH, et al. Glucocorticoid receptor, C/EBP, HNF3, and protein kinase A coordinately activate the glucocorticoid response unit of the carbamoylphosphate synthetase I gene. Mol Cell Biol 1998;18:6305–6315.
6. Christoffels VM, van den Hoff MJ, Moorman AF, et al. The far-upstream enhancer of the carbamoyl-phosphate synthetase I gene is responsible for the tissue specificity and hormone inducibility of its expression. J Biol Chem 1995;270:24932–24940.
7. Hoogenkamp M, Stallen JM, Lamers WH, et al. In vivo footprinting of the carbamoylphosphate synthetase I cAMP-response unit indicates important roles for FoxA and PKA in formation of the enhanceosome. Biochimie 2006;88:1357–1366.
8. Schoneveld OJ, Gaemers IC, Hoogenkamp M, et al. The role of proximal-enhancer elements in the glucocorticoid regulation of carbamoylphosphate synthetase gene transcription from the upstream response unit. Biochimie 2005;87:1033–1040.
9. Kimura T, Christoffels VM, Chowdhury S, et al. Hypoglycemia-associated hyperammonemia caused by impaired expression of ornithine cycle enzyme genes in C/EBPalpha knockout mice. J Biol Chem 1998;273:27505–27510.
10. Matsumoto K, Wolffe AP. Gene regulation by Y-box proteins: coupling control of transcription and translation. Trends Cell Biol 1998;8:318–323.
11. Didier DK, Schiffenbauer J, Woulfe SL, et al. Characterization of the cDNA encoding a protein binding to the major histocompatibility complex class II Y box. Proc Natl Acad Sci U S A 1988;85:7322–7326.
12. Evdokimova V, Ovchinnikov LP, Sorensen PH. Y-box binding protein 1: providing a new angle on translational regulation. Cell Cycle 2006;5:1143–1147.
13. Ise T, Nagatani G, Imamura T, et al. Transcription factor Y-box binding protein 1 binds preferentially to cisplatin-modified DNA and interacts with proliferating cell nuclear antigen. Cancer Res 1999;59:342–346.
14. Kohno K, Izumi H, Uchiumi T, et al. The pleiotropic functions of the Y-box-binding protein, YB-1. Bioessays 2003;25:691–698.
15. Yasen M, Kajino K, Kano S, et al. The up-regulation of Y-box binding proteins (DNA binding protein A and Y-box binding protein-1) as prognostic markers of hepatocellular carcinoma. Clin Cancer Res 2005;11:7354–7361.
16. Inagaki Y, Kushida M, Higashi K, et al. Cell type-specific intervention of transforming growth factor beta/Smad signaling suppresses collagen gene expression and hepatic fibrosis in mice. Gastroenterology 2005;129:259–268.
17. Lu ZH, Books JT, Ley TJ. YB-1 is important for late-stage embryonic development, optimal cellular stress responses, and the prevention of premature senescence. Mol Cell Biol 2005;25:4625–4637.
18. Kamiya A, Kinoshita T, Ito Y, et al. Fetal liver development requires a paracrine action of oncostatin M through the gp130 signal transducer. EMBO J 1999;18:2127–2136.
19. Tanimizu N, Nishikawa M, Saito H, et al. Isolation of hepatoblasts based on the expression of Dlk/Pref-1. J Cell Sci 2003;116:1775–1786.
20. Lee YH, Sauer B, Johnson PF, et al. Disruption of the c/ebp alpha gene in adult mouse liver. Mol Cell Biol 1997;17:6014–6022.
21. Sekine K, Chen YR, Kojima N, et al. Foxo1 links insulin signaling to C/EBPalpha and regulates gluconeogenesis during liver development. EMBO J 2007;26:3607–3615.
22. Nakamura K, Nonaka H, Saito H, et al. Hepatocyte proliferation and tissue remodeling is impaired after liver injury in oncostatin M receptor knockout mice. Hepatology 2004;39:635–644.
23. Kojima N, Kinoshita T, Kamiya A, et al. Cell density-dependent regulation of hepatic development by a gp130-independent pathway. Biochem Biophys Res Commun 2000;277:152–158.
24. Tanimizu N, Miyajima A. Molecular mechanism of liver development and regeneration. Int Rev Cytol 2007;259:1–48.
25. Jurchott K, Bergmann S, Stein U, et al. YB-1 as a cell cycle-regulated transcription factor facilitating cyclin A and cyclin B1 gene expression. J Biol Chem 2003;278:27988–27996.
26. Lagace M, Goping IS, Mueller CR, et al. The carbamyl phosphate synthetase promoter contains multiple binding sites for C/EBP-related proteins. Gene 1992;118:231–238.
27. Meijer AJ, Lamers WH, Chamuleau RA. Nitrogen metabolism and ornithine cycle function. Physiol Rev 1990;70:701–748.
28. Gupta S, Rogers LK, Taylor SK, et al. Inhibition of carbamyl phosphate synthetase-I and glutamine synthetase by hepatotoxic doses of acetaminophen in mice. Toxicol Appl Pharmacol 1997;146:317–327.
29. Bargou RC, Jurchott K, Wagener C, et al. Nuclear localization and increased levels of transcription factor YB-1 in primary human breast cancers are associated with intrinsic MDR1 gene expression. Nat Med 1997;3:447–450.
30. Goping IS, Shore GC. Interactions between repressor and anti-repressor elements in the carbamyl phosphate synthetase I promoter. J Biol Chem 1994;269:3891–3896.
31. Subramanian L, Benson MD, Iniguez-Lluhi JA. A synergy control motif within the attenuator domain of CCAAT/enhancer-binding protein alpha inhibits transcriptional synergy through its PIASy-enhanced modification by SUMO-1 or SUMO-3. J Biol Chem 2003;278:9134–9141.
32. Grant CE, Deeley RG. Cloning and characterization of chicken YB-1: regulation of expression in the liver. Mol Cell Biol 1993;13:4186–4196.
33. Uramoto H, Izumi H, Ise T, et al. p73 Interacts with c-Myc to regulate Y-box-binding protein-1 expression. J Biol Chem 2002;277:31694–31702.

34. Shirota Y, Kaneko S, Honda M, et al. Identification of differentially expressed genes in hepatocellular carcinoma with cDNA microarrays. Hepatology 2001;33:832–840.
35. Schmiedeberg P, Biempica L, Czaja MJ. Timing of protooncogene expression varies in toxin-induced liver regeneration. J Cell Physiol 1993;154:294–300.
36. Fukada T, Tonks NK. Identification of YB-1 as a regulator of PTP1B expression: implications for regulation of insulin and cytokine signaling. EMBO J 2003;22:479–493.

Received June 13, 2008. Accepted February 17, 2009.

Reprint requests

Atsushi Miyajima, Institute of Molecular and Cellular Biosciences, The University of Tokyo, 1-1-1 Yayoi, Bunkyo-ku, Tokyo 113-0032, Japan. e-mail: miyajima@iam.u-tokyo.ac.jp; fax: 81-3-5841-8475.

Acknowledgments

We are grateful to Dr O. Ohara at Kazusa DNA Research Institute for providing us with plasmids, and to Drs T. Itoh and N. Tanimizu for helpful discussions and critical reading of the manuscript.

Conflicts of Interest

The authors disclose no conflicts.

Funding

This work was supported in part by a grant for Core Research for Evolutionary Science and Technology of Japan Science and Technology Agency (JST), and a Grant-in-Aid for Scientific Research and Global COE Program (Integrative Life Science Based on the Study of Biosignaling Mechanisms) from the Ministry of Education, Sports, Science and Technology, Japan.

FEBS Letters 583 (2009) 777–781

FEBS Letters

journal homepage: www.FEBSLetters.org

Inducible expression of *Wnt* genes during adult hepatic stem/progenitor cell response

Tohru Itoh *, Yoshiko Kamiya, Mayuko Okabe [1], Minoru Tanaka, Atsushi Miyajima

Laboratory of Cell Growth and Differentiation, Institute of Molecular and Cellular Biosciences, The University of Tokyo, 1-1-1 Yayoi, Bunkyo-ku, Tokyo 113-0032, Japan

ARTICLE INFO

Article history:
Received 24 November 2008
Revised 12 January 2009
Accepted 16 January 2009
Available online 25 January 2009

Edited by Lukas Huber

Keywords:
Liver regeneration
Oval cell
Wnt
β-Catenin

ABSTRACT

In injured livers where hepatocyte growth is severely limited, facultative hepatic stem/progenitor cells, termed oval cells in rodents, are known to emerge and contribute to the regeneration process. Here, we investigated a possible involvement of Wnt signaling during mouse oval cell response and found significant upregulation of several *Wnt* genes including *Wnt7a*, *Wnt7b*, and *Wnt10a*. Accordingly, increase of β-catenin protein was observed in oval cell compartments. Pharmacological activation of the canonical Wnt/β-catenin signaling induced proliferation of cultured hepatic stem/progenitor cell lines. These results together implicate the role of Wnt/β-catenin signaling in adult hepatic stem/progenitor cell response.

1. Introduction

The liver possesses a unique and remarkable capacity to regenerate upon various injuries, such as those caused by partial hepatectomy or toxic insults. The liver regeneration can usually be achieved by proliferation of the differentiated postmitotic hepatocytes that remain intact, without necessitating an involvement of stem/progenitor cell populations [1]. However, under the severe and/or chronic liver damage conditions where hepatocyte proliferation is suppressed, the facultative stem/progenitor cells are known to emerge and contribute to the regeneration process. Those stem/progenitor cells, referred to as oval cells in rodents, are characterized by their potentials to proliferate as well as to differentiate into both hepatocytes and cholangiocytes, the two epithelial lineages in the liver [2–5]. Despite of their functional relevance in the liver pathophysiology being implicated, the nature and the regulatory mechanisms of the adult hepatic stem/progenitor cells still remain largely unclear.

The Wnt family of secreted factors plays multiple critical roles in regulation of various aspects of liver biology. The Wnt ligands can activate multiple signaling pathways in their target cells, among which the canonical pathway mediated by β-catenin is the best characterized and also highly relevant in stem cell regulation. In the canonical pathway, binding of Wnts to the receptor Frizzled (Fzd) inhibits the kinase GSK3β that normally phosphorylates and primes destruction of the cytoplasmic β-catenin in the absence of ligands, thereby leading to stabilization of the β-catenin proteins, which in turn translocate into the nucleus and mediate transcriptional activation of target genes by forming a complex with the DNA-binding factor TCF/LEF [6,7]. In addition to its role in adult hepatocytes, including liver zonation and hepatic carcinogenesis, the relationship of Wnt/β-catenin signaling with fetal liver stem/progenitor cells in particular have been extensively studied to date and established critical roles of this signaling pathway in controlling proliferation, differentiation, and self-renewal of these cells (reviewed in [8], and references therein; [9]). Recently, activation and possible functional involvement of the Wnt/β-catenin pathway in adult liver stem/progenitor cells have also been implicated by two groups using rodent models of oval cell induction [10,11]. However, detailed time course of its activation with reference to the kinetics of the stem/progenitor cell response was not clarified. Moreover, direct effect of the pathway activation on the adult stem/progenitor cell biology has so far been tested using only one particular cell line.

In this study, we also explored a possible involvement of Wnt/β-catenin signaling in regulation of adult hepatic stem/progenitor cells by employing a mouse oval cell induction model, where administration of the hepatotoxin 3,5-dietoxycarbonyl-1,4-dihydro-collidine (DDC) causes severe chronic liver injury and stimulates emergence and massive proliferation of oval cells [12].

* Corresponding author. Fax: +81 3 5841 8475.
E-mail address: itohru@iam.u-tokyo.ac.jp (T. Itoh).
[1] Present address: Pharmacology Research Labs., Drug Discovery Research, Astellas Pharma Inc., 21 Miyukigaoka, Tsukuba-shi, Ibaraki 305-8585, Japan.

0014-5793/$34.00
doi:10.1016/j.febslet.2009.01.022

2. Materials and methods

2.1. Antibodies and reagents

Polyclonal rabbit anti-CK19 antibody was raised as previously described [13]. Polyclonal rabbit anti-β-catenin antibody and monoclonal mouse anti-β-catenin antibody were obtained from SIGMA and BD Transduction Laboratories, respectively. The GSK3β inhibitor 6-bromoindirubin-3′-oxime (BIO) [14] was kindly synthesized and provided by Drs. Aya Tanatani and Yuichi Hashimoto (IMCB, The University of Tokyo). The inactive analog 1-methyl-BIO (MeBIO, or GSK-3 inhibitor XIV; Calbiochem) was used as a negative control.

2.2. Mice and oval cell induction

C57BL/6 mice were purchased from CLEA Japan, Inc. (Tokyo, Japan) and maintained under a standard SPF condition. All animal experiments were performed with procedures according to the guideline set by the institutional animal care and use committee of the University of Tokyo. Male mice of 8–12 week old were fed 0.1% DDC-containing diet (F-4643; bio serve) to induce hepatic oval cell response, and then killed to harvest liver samples.

2.3. RNA preparation and cDNA synthesis

Total RNA was prepared from whole liver samples homogenized in TRIzol reagent (Invitrogen), treated with DNaseI (Invitrogen), and then used for cDNA synthesis using SuperScript III (Invitrogen) with random hexamer primers.

2.4. PCR analyses

Standard PCR reactions were performed with Blend Taq (TOYOBO), and the products were run in 1.5% agarose gels and visualized with EtBr staining. Quantitative PCR analyses were done using LightCycler (Roche) with SYBR Premix Ex Taq reagent (TaKaRa). *Gapdh* was used as an internal control. The primers used are summarized in Supplementary data.

2.5. Immunohistochemistry

The fresh liver samples were fixed in Zamboni's fixative solution and embedded in OCT compound (Sakura Finetek Japan Co. Ltd., Tokyo, Japan). The samples were frozen and sectioned onto APS-coated glass slides (Matsunami Glass Ind. Ltd., Osaka, Japan). After blocking in 5% skim milk/PBS, the samples were incubated with primary antibodies and then with fluorescence-conjugated secondary antibodies. Nuclei were counterstained with Hoechst 33342 (Sigma).

2.6. Cell culture and proliferation assay

The hepatic stem/progenitor cell lines, HSCEs, as well as their precedent bulk culture of the EpCAM$^+$ cell-derived fraction, were maintained in type I collagen-coated dishes using a medium supplemented with 10 ng/ml each of recombinant human EGF and HGF (see Supplementary data). The detail for their establishment and characterization will be described elsewhere (Okabe et al., submitted).

Proliferative response of HSCE cells was examined by a colorimetric assay using WST-1 cell proliferation reagent (Roche)

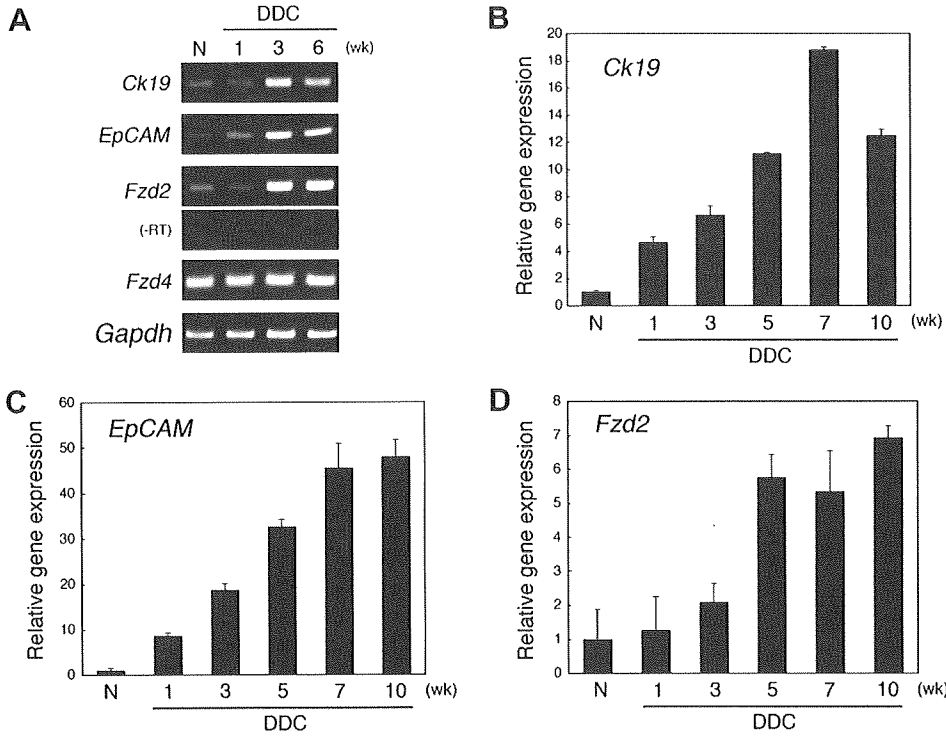

Fig. 1. Expression of *Fzd2* is upregulated in the livers of DDC diet-fed mice concomitantly with the oval cell marker genes. (A) Total RNA was isolated from whole liver samples of normal diet-fed (N) and DDC diet-fed mice, reverse-transcribed, and subjected to PCR analyses to determine expression of *Fzd2*, *Fzd4*, the oval cell markers *Ck19* and *EpCAM*, and *Gapdh*. Note that the primer sets used to detect *Fzd4*, *Ck19*, *EpCAM*, and *Gapdh* were designed to flank one or more intron(s). For the Fzd2 gene, which comprises only of one exon, control RNA samples without reverse transcription (-RT) were also examined, confirming no adverse amplification caused by contaminated genomic DNA. (B) Inducible expression of *Fzd2*, *Ck19*, and *EpCAM* were analyzed by quantitative PCR analyses. Expression was normalized to that of *Gapdh*.

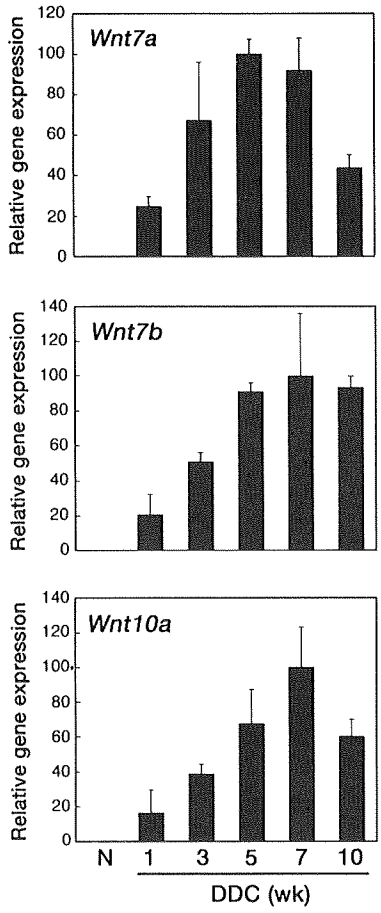

Fig. 2. Inducible expression of *Wnt7a*, *Wnt7b*, and *Wnt10a* in the livers of DDC diet-fed mice. Expression of *Wnt7a*, *Wnt7b*, and *Wnt10a* during the course of oval cell induction was analyzed by quantitative PCR analyses. Expression was normalized to that of *Gapdh*.

according to the manufacturer's protocol. The absorbance value (OD_{450}–OD_{650}) was measured using an Emax microplate reader (Molecular Devices).

2.7. Transfection and luciferase assay

HSCE5 cells were transfected with the TOPtkLuciferase or FOPtkLuciferase plasmid using Lipofectamine with Plus reagent (Invitrogen), and cultured in the presence or absence of the GSK3 inhibitor BIO for 48 h. The cells were lysed in Passive Lysis Buffer (Promega) and subjected to a luciferase assay using a luminometer (MICROLUMAT LB96P; Berthold) with Dual luciferase assay reagent (Promega).

3. Results and discussion

We recently performed a screening project that aimed to isolate cell surface molecules expressed in oval cells, and identified EpCAM as a novel marker for mouse oval cells (Okabe et al., submitted). Notably, EpCAM was recently reported to be a marker for rat oval cells [15]. In the same screening, we also noticed two Frizzled (Fzd) family members, Fzd2 and Fzd4, as molecules expressed in the oval cell-induced rat livers. To explore the possible involvement of these Fzd molecules in oval cell biology, we examined their expression in the mouse DDC diet model for oval cell induction. As shown in Fig. 1A, feeding with DDC diet resulted in oval cell induction in mice, as manifested by strong upregulation of the oval cell marker genes *CK19* as well as *EpCAM*. Basal expression of these genes in the normal liver derived from cholangiocytes, which are known to express these markers as well. During the course of oval cell induction, *Fzd2* also was strongly upregulated. Expression of *Fzd4*, although apparently observed in DDC diet-fed samples, was not inducible but rather constant. Quantitative PCR analyses further confirmed that *Fzd2*, like *CK19* and *EpCAM*, was highly upregulated in oval cell-induced mouse livers (Fig. 1B–D).

The Frizzled family molecules including Fzd2 function as the receptor component for the Wnt family ligands, which prompted us to investigate possible induction of the *Wnt* genes in the oval cell-induced livers. We compared expression of all the 19 members of the mouse *Wnt* genes and found that several of them were significantly upregulated in the livers of DDC diet-fed mice (Fig. S1A). Specifically, *Wnt7a*, *Wnt7b*, and *Wnt10a* showed strong upregulation with more than 50-fold increase above the basal level in the normal livers. We further examined the time course of expression of those *Wnt* genes and confirmed that their induction kinetics was well correlated with that of the oval cell appearance (Fig. 2; com-

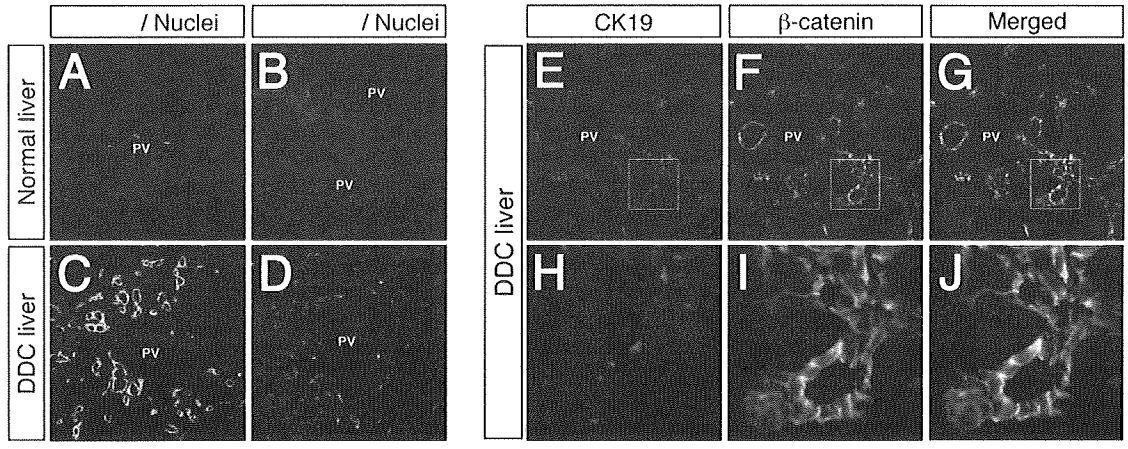

Fig. 3. β-catenin proteins are increased in oval cells. A–D. Liver sections prepared from a normal control mouse (A and B) and a DDC diet-fed mouse (5 wk; C and D) were subjected to immunofluorescent staining analyses using anti-CK19 (A and C) and anti-β-catenin (B and D) antibodies (Green). Nuclei were counterstained with Hoechst 33342 (Blue). E–J. Double staining experiments were performed to confirm co-expression of CK19 (E and H) and β-catenin (F and I) in the livers of the oval cell-induced mice. Panels G and J shows the merged images, where nuclear staining by Hoechst 33342 is also included (Blue). Panels H–J provide higher power images corresponding to the squared regions in panels E–G, respectively. PV, portal vein.

pare with Fig. 1B and C). For comparison, we also monitored expression kinetics of *Wnt3* and *Wnt3a*, two representative members of the canonical Wnt ligands, and found that neither of them was expressed during the course of oval cell induction up to 10 weeks.

It has been reported that Wnt7a, Wnt7b, and Wnt10a are all capable of activating the canonical signaling pathway [16–19]. As a well-established hallmark of the canonical Wnt signal activation is stabilization and accumulation of β-catenin, we performed immunostaining analyses of this molecule using liver sections (Fig. 3). β-Catenin is a component of the cell adhesion complex in every hepatocyte, so that staining of the normal liver samples detected its basal level expression with a relatively uniform distribution pattern (Fig. 3B). In damaged livers, oval cells are known to emerge from periportal regions, forming duct-like structures, which was readily detectable based on expression of the marker molecule CK19 (Fig. 3C). Remarkably, those propagating oval cells were strongly positive for anti-β-catenin immunostaining (Fig. 3D). Double staining experiments confirmed that the intense β-catenin signals indeed co-localized with CK19 expression in the same cells (Fig. 3E–J). Although the signals appeared most intense at and adjacent to the cell membrane, weaker yet significant signals were also observed diffusively throughout the cytoplasm as well as in the nucleus in some if not all cells. It should be noted that, in many cases, cells that undergo Wnt signaling may display an overall rise in β-catenin protein without a clear nuclear preference [6]. These results suggest that the induced expression of Wnt ligands leads to concomitant activation of the canonical signaling pathway in oval cells.

The canonical Wnt signaling stimulates transcriptional activation of various target genes. To further confirm that the canonical pathway is indeed turned on and functioning in oval cells, we assessed induction of known target genes in the oval cell-induced livers. Using fractionated cell samples derived from the livers of DDC diet-fed mice, we observed that several of the known targets, including *Axin2*, *N-myc*, and *Wisp1*, were significantly upregulated predominantly in the EpCAM$^+$ oval cell population (Fig. S2). Moreover, a recent study has reported that the oval cell marker EpCAM is itself a direct transcriptional target of Wnt/β-catenin pathway [20]. Together, these facts further support the notion that the canonical pathway is functionally activated in oval cells.

To gain an insight into the role that active Wnt/β-catenin signaling plays in oval cell regulation, we examined whether this could affect proliferation of hepatic stem/progenitor cells *in vitro*. The bi-potential adult hepatic stem/progenitor cell lines, referred to as HSCEs, were originally established from the EpCAM$^+$ oval cell fraction in the livers of DDC diet-fed mice, and is capable of proliferating in the presence of EGF and HGF (Okabe et al., submitted). RT-PCR analyses revealed that a representative clone of HSCE (clone 5; HSCE5) expresses several members of the Fzd family receptors, as well as the co-receptors Lrp5/6 (Fig. S3), suggesting that the cells could respond to Wnt stimulation *per se*. We employed a small compound GSK3β inhibitor, BIO, which has been shown to be capable of mimicking activation of the canonical pathway by suppressing GSK3β-mediated phosphorylation and concomitant degradation of β-catenin [14]. Stimulation with BIO indeed led to activation of the canonical pathway in HSCE5, as demonstrated by induction of the β-catenin/TCF-dependent TOPtkLuciferase reporter activity (Fig. 4A). We then tested the effect of BIO on proliferation of HSCE5, and found that application of the compound did induce significant proliferative response of the cells even in the absence of EGF and HGF, to a level nearly comparable to the one induced by these cytokines (Fig. 4B). Application of 5 mM of BIO resulted in a less effect, due presumably to its cyto-

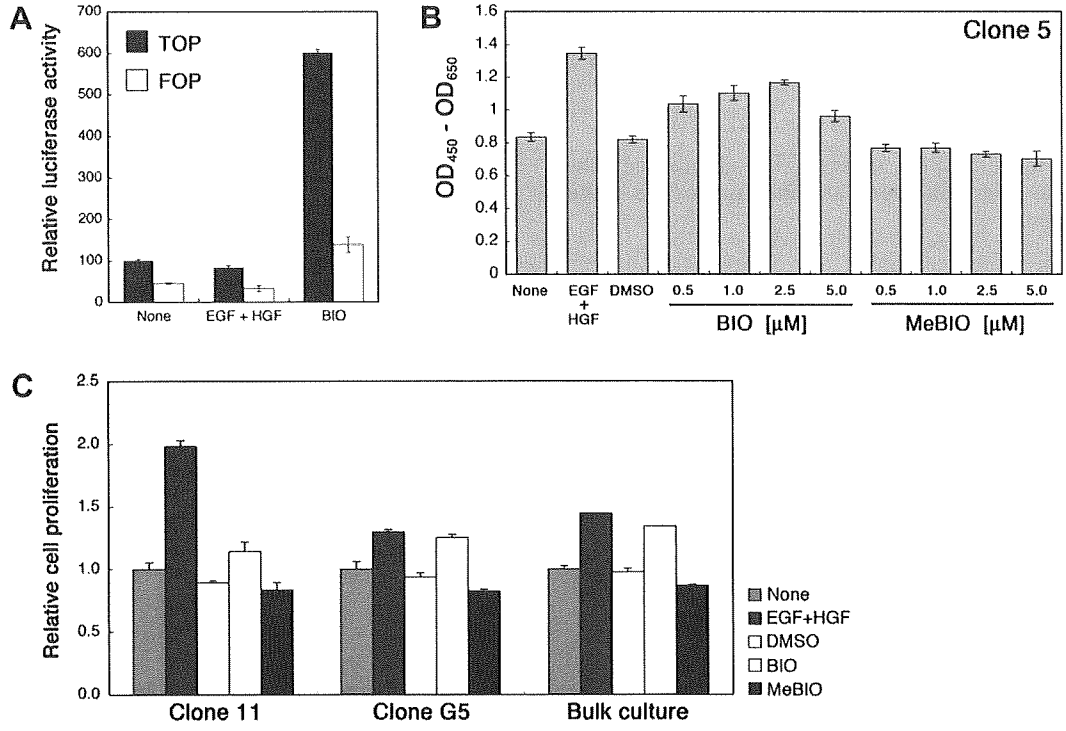

Fig. 4. Pharmacological activation of Wnt/β-catenin signaling stimulates proliferation of the adult hepatic stem/progenitor cell lines HSCE. (A) HSCE5 cells were transfected with TOPtkLuciferase (TOP; a reporter for canonical Wnt signaling activity) or FOPtkLuciferase (FOP; an unresponsive control), cultured in the presence or absence of the GSK3 inhibitor BIO, and then subjected to a luciferase assay. Stimulation with EGF and HGF was used as a control. (B) HSCE5 cells were plated in a 96-well plate at a density of 2.5×10^3 cells/well, and cultured in the presence or absence of BIO, its inactive analog MeBIO, or the vehicle (DMSO). Stimulation with EGF and HGF was used as a control. After 48 hours of incubation, the level of cell proliferation was examined by WST-1 assay. (C) Proliferative response of additional HSCE cell lines (clones 11 and G5), as well as the bulk culture of the EpCAM$^+$ cell fraction-derived cells before being subjected to clonal isolation of HSCE cell lines, were examined by WST-1 assay as in (B). Note that the clone G5 harbors the retrovirally-transduced GFP marker gene.

toxicity at this dose. The inactive analog MeBIO was used as a negative control, showing no obvious effect. Finally, we tested the effect of the compounds on other independent clones of HSCE, as well as on the bulk culture of the $EpCAM^+$ cell fraction-derived cells before being subjected to clonal isolation of HSCE cell lines. As shown in Fig. 4C, all of them were capable of responding to stimulation with BIO, resulting in significant proliferative induction.

In addition to the β-catenin-dependent canonical signaling pathway, some Wnt ligands can activate non-canonical signaling pathways, such as the planar cell polarity/c-Jun N-terminal kinase (JNK) pathway and the Ca^{2+}-mediated pathway [21]. Notably, it has been reported that Wnt7a and Wnt7b can activate the JNK pathway in endometrial cancer cells and hippocampal neurons, respectively [22,23], while Fzd2 has been shown to mediate activation of non-canonical signaling pathways in certain types of cells [21,24–26]. Although our results have clearly established activation of the canonical pathway *in vivo* and its functional effect *in vitro*, a possible involvement of the non-canonical pathways in oval cell regulation cannot be neglected and should also be addressed in future studies.

In summary, our present study has identified several Wnt ligands and the downstream canonical signaling pathway as a possible regulatory signal for mouse oval cells, a well-recognized facultative stem/progenitor cell population in the adult liver. Much progress has been made in recent years in identifying and characterizing various tissue stem cells as well as their specialized surrounding microenvironments, or stem cell niches. The niches play fundamental roles in controlling proliferation, differentiation, and/or self-renewal of the stem cells through direct cell–cell interactions and also via various soluble cytokines, such as Wnts, Hedgehogs, and BMPs [27,28]. Although it still remains unknown whether any niche structures are formed to support hepatic oval cells, it is tempting to speculate that Wnt/β-catenin signaling may play a role as a part of the niche signals in regulating their development and behaviors.

Acknowledgments

We are grateful to Drs. Aya Tanatani and Yuichi Hashimoto (IMCB, The University of Tokyo, Japan) for kindly providing the synthetic GSK3β inhibitor BIO, and Dr. Eiko Saijou and Ms. Hinako Takase for help with qPCR analyses. This work was supported in part by Grants-in-Aid for Scientific Research from the Ministry of Education, Culture, Sports, Science and Technology of Japan (17014016) and from the CREST program of Japan Science and Technology Agency.

Appendix A. Supplementary data

Supplementary data associated with this article can be found, in the online version, at doi:10.1016/j.febslet.2009.01.022.

References

[1] Michalopoulos, G.K. and DeFrances, M.C. (1997) Liver regeneration. Science 276, 60–66.
[2] Grompe, M. and Finegold, M. (2001) Liver stem cells in: Stem Cell Biology (Marshak, D.R., Gardner, R.L. and Gottlieb, D., Eds.), pp. 455–497, Cold Spring Harbor Laboratory Press, Cold Spring Harbor, New York.
[3] Fausto, N. (2004) Liver regeneration and repair: hepatocytes, progenitor cells, and stem cells. Hepatology 39, 1477–1487.
[4] Matthews, V.B. and Yeoh, G.C. (2005) Liver stem cells. IUBMB Life 57, 549–553.
[5] Bird, T.G., Lorenzini, S. and Forbes, S.J. (2008) Activation of stem cells in hepatic diseases. Cell Tissue Res. 331, 283–300.
[6] Clevers, H. (2006) Wnt/beta-catenin signaling in development and disease. Cell 127, 469–480.
[7] Macdonald, B.T., Semenov, M.V. and He, X. (2007) SnapShot: Wnt/beta-catenin signaling. Cell 131, 1204.
[8] Thompson, M.D. and Monga, S.P. (2007) WNT/beta-catenin signaling in liver health and disease. Hepatology 45, 1298–1305.
[9] Chiba, T. et al. (2007) Enhanced self-renewal capability in hepatic stem/progenitor cells drives cancer initiation. Gastroenterology 133, 937–950.
[10] Apte, U., Thompson, M.D., Cui, S., Liu, B., Cieply, B. and Monga, S.P. (2008) Wnt/beta-catenin signaling mediates oval cell response in rodents. Hepatology 47, 288–295.
[11] Hu, M., Kurobe, M., Jeong, Y.J., Fuerer, C., Ghole, S., Nusse, R. and Sylvester, K.G. (2007) Wnt/beta-catenin signaling in murine hepatic transit amplifying progenitor cells. Gastroenterology 133, 1579–1591.
[12] Preisegger, K.H., Factor, V.M., Fuchsbichler, A., Stumptner, C., Denk, H. and Thorgeirsson, S.S. (1999) Atypical ductular proliferation and its inhibition by transforming growth factor beta1 in the 3,5-diethoxycarbonyl-1,4-dihydrocollidine mouse model for chronic alcoholic liver disease. Lab. Invest. 79, 103–109.
[13] Tanimizu, N., Nishikawa, M., Saito, H., Tsujimura, T. and Miyajima, A. (2003) Isolation of hepatoblasts based on the expression of Dlk/Pref-1. J. Cell Sci. 116, 1775–1786.
[14] Meijer, L. et al. (2003) GSK-3-selective inhibitors derived from Tyrian purple indirubins. Chem. Biol. 10, 1255–1266.
[15] Yovchev, M.I., Grozdanov, P.N., Joseph, B., Gupta, S. and Dabeva, M.D. (2007) Novel hepatic progenitor cell surface markers in the adult rat liver. Hepatology 45, 139–149.
[16] Hirabayashi, Y., Itoh, Y., Tabata, H., Nakajima, K., Akiyama, T., Masuyama, N. and Gotoh, Y. (2004) The Wnt/beta-catenin pathway directs neuronal differentiation of cortical neural precursor cells. Development 131, 2791–2801.
[17] Maye, P., Zheng, J., Li, L. and Wu, D. (2004) Multiple mechanisms for Wnt11-mediated repression of the canonical Wnt signaling pathway. J. Biol. Chem. 279, 24659–24665.
[18] Narita, T., Sasaoka, S., Udagawa, K., Ohyama, T., Wada, N., Nishimatsu, S., Takada, S. and Nohno, T. (2005) Wnt10a is involved in AER formation during chick limb development. Dev. Dyn. 233, 282–287.
[19] Wang, Z., Shu, W., Lu, M.M. and Morrisey, E.E. (2005) Wnt7b activates canonical signaling in epithelial and vascular smooth muscle cells through interactions with Fzd1, Fzd10, and LRP5. Mol. Cell Biol. 25, 5022–5030.
[20] Yamashita, T., Budhu, A., Forgues, M. and Wang, X.W. (2007) Activation of hepatic stem cell marker EpCAM by Wnt-beta-catenin signaling in hepatocellular carcinoma. Cancer Res. 67, 10831–10839.
[21] Semenov, M.V., Habas, R., Macdonald, B.T. and He, X. (2007) SnapShot: Noncanonical Wnt signaling pathways. Cell 131, 1378.
[22] Carmon, K.S. and Loose, D.S. (2008) Secreted frizzled-related protein 4 regulates two Wnt7a signaling pathways and inhibits proliferation in endometrial cancer cells. Mol. Cancer Res. 6, 1017–1028.
[23] Rosso, S.B., Sussman, D., Wynshaw-Boris, A. and Salinas, P.C. (2005) Wnt signaling through Dishevelled, Rac and JNK regulates dendritic development. Nat. Neurosci. 8, 34–42.
[24] Slusarski, D.C., Corces, V.G. and Moon, R.T. (1997) Interaction of Wnt and a Frizzled homologue triggers G-protein-linked phosphatidylinositol signalling. Nature 390, 410–413.
[25] Ishitani, T. et al. (2003) The TAK1-NLK mitogen-activated protein kinase cascade functions in the Wnt-5a/Ca(2+) pathway to antagonize Wnt/beta-catenin signaling. Mol. Cell Biol. 23, 131–139.
[26] Wang, H.Y. and Malbon, C.C. (2003) Wnt signaling, Ca^{2+}, and cyclic GMP: visualizing Frizzled functions. Science 300, 1529–1530.
[27] Jones, D.L. and Wagers, A.J. (2008) No place like home: anatomy and function of the stem cell niche. Nat. Rev. Mol. Cell Biol. 9, 11–21.
[28] Moore, K.A. and Lemischka, I.R. (2006) Stem cells and their niches. Science 311, 1880–1885.

Development 136, 1951-1960 (2009) doi:10.1242/dev.031369

Potential hepatic stem cells reside in EpCAM$^+$ cells of normal and injured mouse liver

Mayuko Okabe[1,*], Yuko Tsukahara[1,*], Minoru Tanaka[1,*,†], Kaori Suzuki[1], Shigeru Saito[1], Yoshiko Kamiya[1], Tohru Tsujimura[2], Koji Nakamura[3] and Atsushi Miyajima[1]

Hepatic oval cells are considered to be facultative hepatic stem cells (HSCs) that differentiate into hepatocytes and cholangiocytes in severely injured liver. Hepatic oval cells have also been implicated in tumorigenesis. However, their nature and origin remain elusive. To isolate and characterize mouse oval cells, we searched for cell surface molecules expressed on oval cells and analyzed their nature at the single-cell level by flow cytometric analysis and in the in vitro colony formation assay. We demonstrate that epithelial cell adhesion molecule (EpCAM) is expressed in both mouse normal cholangiocytes and oval cells, whereas its related protein, TROP2, is expressed exclusively in oval cells, establishing TROP2 as a novel marker to distinguish oval cells from normal cholangiocytes. EpCAM$^+$ cells isolated from injured liver proliferate to form colonies in vitro, and the clonally expanded cells differentiate into hepatocytes and cholangiocytes, suggesting that the oval cell fraction contains potential HSCs. Interestingly, such cells with HSC characteristics exist among EpCAM$^+$ cells of normal liver. Intriguingly, comparison of the colony formation of EpCAM$^+$ cells in normal and injured liver reveals little difference in the number of potential HSCs, strongly suggesting that most proliferating mouse oval cells represent transit-amplifying cells rather than HSCs.

KEY WORDS: Hepatic stem cell, Oval cell, EpCAM, TROP2 (TACSTD2), Hepatocyte, Cholangiocyte, Liver injury

INTRODUCTION

Most of the metabolic functions in the liver are carried out by hepatocytes that form hepatic cords, whereas cholangiocytes form bile ducts that drain bile produced by hepatocytes. During development, hepatocytes and cholangiocytes, two types of hepatic epithelial cells, derive from hepatoblasts emerging from the foregut endoderm (Notenboom et al., 2003; Zaret, 2000). Hepatoblasts are highly proliferative and express hepatocytic proteins such as albumin (ALB) and alpha-fetoprotein (AFP), an immature hepatocyte marker. As the liver develops, hepatoblasts propagate and those close to the portal mesenchyme differentiate into cholangiocytes, while the rest become mature hepatocytes (Lemaigre, 2003). Therefore, hepatoblasts are thought to be hepatic stem/progenitor cells in the fetus.

By contrast, it is highly controversial whether adult mammalian liver contains hepatic stem cells (HSCs). Adult liver has a remarkable potential to regenerate from severe parenchymal loss, even though hepatocytes and cholangiocytes are mitotically dormant under normal conditions. Hepatocytes have a remarkable potential to self-replicate (Fausto, 2004; Michalopoulos and DeFrances, 1997) and are capable of at least 80 doublings by serial transplantation (Overturf et al., 1997), allowing the liver to regenerate. However, liver injury that limits this pathway accompanies the proliferation of a potential stem/progenitor cell compartment at the interface of the biliary tree and hepatic cords, which is known as the ductular reaction (Alison et al., 1996; Roskams et al., 2004; Theise et al., 1999). These undifferentiated epithelial cells are often referred to as 'oval cells' because of their ovoid nucleus (Farber, 1956). Upon activation, oval cells expand into liver parenchyma from the portal area. Oval cells express both ALB and cytokeratin 19 (CK19; KRT19 – Mouse Genome Informatics), which are hepatocytic and cholangiocytic markers, respectively, and are believed to differentiate into hepatocytic and biliary lineages, similar to hepatoblasts in embryonic liver. Thus, oval cells are thought to be facultative stem/progenitor cells in adult liver. Although oval cells have been most extensively studied in rodents, similar cells have been found in connection with various human liver diseases and are implicated in tumorigenesis (Fausto, 2004; Lee et al., 2006). Whether oval cells constitute HSCs has been debated in numerous reports involving various rodent injury models using chemical reagents, including carcinogenic agents. The 2-acetylaminofluorene (2-AAF)/partial hepatectomy (PH) model, in which hepatocyte proliferation is blocked by 2-AFF prior to PH, has been extensively used to characterize oval cells in rats (Evarts et al., 1987; Laishes and Rolfe, 1981). However, the same procedure does not generate oval cells in mice and alternatives such as the use of a choline-deficient ethionine-supplemented diet (Akhurst et al., 2001) and a 3,5-diethoxycarbonyl-1,4-dihydro-collidine (DDC)-containing diet (Preisegger et al., 1999; Wang et al., 2003) have been developed. Although the proliferating epithelial cells that are present in the periportal region upon injury caused by various insults are referred to as oval cells, it remains unclear whether oval cells generated via different protocols in different species have the same characteristics. A major problem in characterizing oval cells is the lack of appropriate cell surface markers to identify and isolate the oval cell compartment. Therefore, despite a large number of studies, the exact nature of oval cells – including their origin, stemness and bi-directional differentiation – is still poorly understood. Because of the difficulty in performing clonal analysis of HSCs, it has also been unclear whether HSCs exist in normal liver.

The aim of this study was to identify cell surface molecules on mouse oval cells and to analyze their nature at the clonal level. To this end, we utilized the 2-AAF/PH rat model and the DDC diet

[1]Laboratory of Cell Growth and Differentiation, Institute of Molecular and Cellular Biosciences, The University of Tokyo, Tokyo 113-0032, Japan. [2]Department of Pathology, Hyogo College of Medicine, Nishinomiya, Hyogo 663-8501, Japan. [3]LivTech, Miyamae-ku, Kawasaki, Kanagawa 216-0001, Japan.

*These authors contributed equally to this work
[†]Author for correspondence (e-mail: tanaka@iam.u-tokyo.ac.jp)

Accepted 31 March 2009

mouse model to generate oval cells and found that epithelial cell adhesion molecule (EpCAM) and the related molecule, TROP2 (TACSTD2), were upregulated in these livers. EpCAM was expressed in normal cholangiocytes and also in oval cells in the liver of mice fed the DDC diet (DDC liver). By contrast, TROP2 was expressed in almost all $EpCAM^+$ cells in DDC liver, but not in normal liver, indicating that TROP2 is a novel marker to distinguish between normal cholangiocytes and oval cells. Furthermore, we isolated $EpCAM^+$ cells from DDC liver and demonstrated that clonally expanded cells were able to differentiate into hepatocytes and cholangiocytes. Finally, we provide evidence for the presence of potential HSCs in $EpCAM^+$ cells of normal liver and compare their characteristics before and after oval cell activation.

MATERIALS AND METHODS

Animals

C57BL/6 mice (Japan SLC, Hamamatsu, Japan) at 8-12 weeks were used for all experiments. All experiments with animals were performed according to institutional guidelines. The diet containing 0.1% DDC was purchased from CLEA, Japan. Mouse oval cells were activated by feeding with the diet containing 0.1% DDC.

Identification of cDNA encoding a membrane protein

Total RNA was prepared from the non-parenchymal fraction of rat liver treated with 2-AAF/PH at 7 days after PH as described previously (Tanimizu et al., 2004b). Total RNA was amplified using the MessageAmp aRNA Amplification Kit (Ambion), and used to construct a cDNA library in the pMXs-SST vector using the SuperScript Choice System (Invitrogen, Carlsbad, CA, USA). The cDNA library contained 4.3×10^6 independent clones. The signal sequence trap method was performed as described previously (Kojima and Kitamura, 1999).

Preparation of liver cells and flow cytometry (FCM)

A single-cell suspension from DDC and normal livers was obtained by a modified two-step collagenase perfusion method as described previously (Seglen, 1976). In short, livers were perfused with liver perfusion medium (Invitrogen) at a flow rate of 3 ml/minute for 5 minutes. Then, the liver was perfused with basic perfusion solution (136 mM NaCl, 5.4 mM KCl, 5 mM $CaCl_2$, 0.5 mM NaH_2PO_3 $2H_2O$, 0.42 mM Na_2HPO_3 $12H_2O$, 10 mM HEPES pH 7.5, 5 mM glucose and 4.2 mM $NaHCO_3$) containing 0.5 g/l collagenase type IV (Sigma, St Louis, MO, USA) at a flow rate of 3 ml/minute for 8 minutes. The digested liver was transferred to a glass dish and chopped into small pieces using a surgical knife in D-PBS (Dulbecco's phosphate-buffered saline). Cells dispersed by pipetting were passed through a 70-μm cell strainer and the flow-through fraction was used for the next step as the first cell suspension. The undigested clot on the strainer was recovered and redigested with basic perfusion solution containing 0.5 g/l collagenase type IV, 0.5 g/l pronase (Roche Diagnostics) and 50 mg/l DNase I (Sigma) by stirring for 20 minutes at 37°C. This digested liver was also passed through a 70-μm cell strainer and the flow-through fraction was combined with the first cell suspension. After centrifugation at 700 rpm (100 *g*) for 2 minutes, the supernatant was transferred to a new tube and the centrifugation repeated until no cell pellet was visible. The final supernatant was centrifuged at 1200 rpm (300 *g*) for 5 minutes and the precipitated cells were used as non-parenchymal cells (NPCs) for FCM analysis. Aliquots of cells were blocked with anti-FcR antibody, co-stained with fluorescein- and biotin-conjugated antibodies, washed, incubated with allophycocyamin-conjugated streptavidin (Invitrogen), and analyzed by FACSCalibur (Becton Dickinson). Dead cells were excluded by propidium iodide staining.

Antibodies and immunohistochemistry (IHC)

The anti-EpCAM monoclonal antibody was generated by immunization of a rat with a Ba/F3 cell transfectant overexpressing EpCAM cDNA. The establishment of hybridoma clones was performed as described previously (Hara et al., 1999). The anti-EpCAM monoclonal antibody was biotinylated using Amersham ECL Protein Biotinylation Module (GE Healthcare, UK) or fluorescein-conjugated using the Fluorescein Labeling Kit-NH_2 (Dojindo Molecular Technologies), and then used for all FCM analyses. The rabbit anti-mouse CK19 polyclonal antibody was raised against the C-terminal peptide, HYNNLPTPKAI, and the serum was used for IHC as previously described (Tanimizu et al., 2003). The biotin-conjugated anti-mouse TROP2 antibody was purchased from R&D Systems. The anti-human Ki67 antibody was purchased from Becton Dickinson. Frozen sections (8 μm) of livers were prepared using a HM505E cryostat (Microm International) after fixation with 4% paraformaldehyde, and incubated with each antibody, followed by a biotin- or fluorescein-conjugated secondary antibody. The signals were visualized by fluorescence microscopy.

RNA extraction and reverse transcription PCR (RT-PCR)

Total RNA was extracted from each cell preparation using Trizol reagent (Invitrogen). Total RNA (1 μg) and random hexamer primers were used to synthesize cDNA using the First-Strand cDNA Synthesis Kit (Amersham Pharmacia Biotech). The samples were denatured at 94°C for 5 minutes, then subjected to 25-40 cycles of denaturation at 94°C for 30 seconds, annealing at 52-57°C for 30 seconds, and extension at 72°C for 1 minute, with the final extension at 72°C for 5 minutes. PCR primers for mouse genes are shown in Table 1. The quantitative real-time RT-PCR was performed using a LightCycler ST300 (Roche) and the following primers (5′ to 3′): rat *Epcam*, TCTACAAGGAAGAGATCAGCAAAA and TGTGTATC-TCACCCATCTCCTTT; rat *Trop2*, GACCAAATGTGTTGGCCTGT and GTCACAGCTGGGAGGAAAAT; rat *Hprt*, GACCGGTTCTGT-CATGTCG and ACCTGGTTCATCATCACTAATCAC.

Table 1. Oligonucleotides used in RT-PCR

Gene	Forward (5′ to 3′)	Reverse (5′ to 3′)
Epcam	CGGCTCAGAGAGACTGTGTC	GATCCAGTAGGTCCTCACGC
Ck19	GTCCTACAGATTGACAATG	CACGCTCTGGATCTGTGACAG
Ck7	GGGATGACCTCCGCAACACC	CTCCAGCAGCTTGCGGTAGG
Alb	CATGACACCATGCCTGCTGAT	GCCTTTCCACCAGGGATCCAC
Afp	CTGGAGTGTCTGCAGGATGG	CCACAGCCGGACCATTTCTC
Gapdh	GGAGCGAGACCCCACTAA	GTGTAGCCCAAGATGCCC
Hprt	GACTGAAAGACTTGCTCGAG	CCAGCAAGCTTGCAACCTTAACAA
G6Pase	AACCCATTGTGAGGCCAGAGG	TACTCATTACACTAGTTGGTC
Tat	TGCATCCTCCTGAAGACATG	CTTCTCTCTGGTGTAGCTCT
Cps	ACTGAGAGATGCTGACCCTA	CCTGGAAATTGGTGAGGAGA
integrin β4	GACCTATGAAGAAGGTGCTC	GGCTCAGATGCGTGCCATAG
Ggt1	GCTGAGCTGATTGAGCATCCG	GGTTGATGAAGTTGGGCGAGC
mucin 1	GAGCGCCAGCCTTGAGTTTG	GGAGGCACTACTGTGGACTG
Trop2	CTGACCTAGACTCCGAGCTG	CCAACCCATCTGGTCTGAGG
claudin 4	GACTTTGACCCCTGCAGAGG	GGCCACAGGCTGTTATGAGC
Cd44	CAGAGGCGACTAGATCCCTC	GAGTCACAGTGCGGGAACTC
Slc10a1	AGATCAAGGCTCACTTCTGG	AGAAGTCCTTCTGCAAGCTG
Tdo2	ACAATGAAGAAGACAGAGC	TGTAGTCTCCTCCAAAGTTA

Culture of EpCAM$^+$ cells and colony formation assay

NPCs were prepared as described above. EpCAM$^+$ cells were sorted by FACSVantage SE (Becton Dickinson). The cells were suspended in the standard medium (Williams' medium E containing 10% FBS, 10 mM nicotinamide, 2 mM L-glutamine, 0.2 mM ascorbic acid, 20 mM HEPES pH 7.5, 1 mM sodium pyruvate, 17.6 mM $NaHCO_3$, 14 mM glucose, 100 nM dexamethasone, 1× ITS (insulin, transferrin, selenium X) and 50 mg/ml gentamicin) and seeded on a type-I collagen-coated dish. human EGF, human recombinant HGF and mouse IL6 were added to the culture to a final concentration of 10 ng/ml each. After the establishment of cell lines, IL6 was excluded from the culture medium because it was confirmed to have no apparent effect. For colony formation assays, EpCAM$^+$ cells were sorted by a two-step selection (see Fig. S1 in the supplementary material) and plated at 1×10^4 cells per 35-mm dish. The isolated cells were cultured for 9 days and then the number and size of colonies were counted.

Differentiation into the hepatocytic lineage in vitro

Clonally expanded cells (3×10^5 per well) were cultured in the standard culture medium in a 6-well plate. After 2 days, 20 ng/ml Oncostatin M (OSM) and 1% DMSO were added into the confluent culture. After 5 days, the medium was changed to standard culture medium containing 20 ng/ml OSM, 1% DMSO and 17% Matrigel (growth factor reduced). After 3 and 5 days, the cultured cells were used for RNA preparation and periodic acid-Schiff (PAS) staining as described (Kamiya et al., 1999).

In vitro differentiation into the cholangiocytic lineage

Cellmatrix Type I-A (Nitta Gelatin) was used for three-dimensional culture to induce cholangiocytic differentiation according to the manufacturer's instructions. In short, 0.3% Cellmatrix Type I-A, a 5× DMEM containing 250 mg/ml gentamicin, and the reconstitution buffer (0.05 M NaOH, 200 mM HEPES pH 7.5, 262 mM $NaHCO_3$) were mixed at a ratio of 7:2:1. This mixture was mixed with an equal volume of 5×10^4 cells suspended in standard culture medium without dexamethasone and nicotinamide but with human recombinant HGF (20 ng/ml). The cell suspension was poured into a 6-well plate and left at 37°C to form a gel. Then, the culture medium was gently laid onto the gel.

RESULTS

Screening for cell surface markers of oval cells

To identify the cell surface molecules expressed on hepatic oval cells, we utilized the signal sequence trap (SST) method, which can efficiently isolate genes encoding a protein with a signal sequence (Kojima and Kitamura, 1999; Watanabe et al., 2007). As there are several protocols for generating oval cells in rats and mice, the characteristics of oval cells might not be the uniform. We therefore searched for cell surface molecules expressed on oval cells in the two species using different protocols (see Fig. S2 in the supplementary material). To this end, we first constructed an SST cDNA library from non-parenchymal cells (NPCs) of rat liver subjected to 2-AAF/PH treatment and identified 54 membrane proteins (see Table S1 in the supplementary material). First, we compared the expression of their counterpart genes for mouse between normal and DDC liver by RT-PCR, and found that *Epcam*, *Trop2*, mucin 1, claudin 4, *Cd44*, integrin β3, *Lyve1*, *gp130* (*Il6st*) and *Fxyd5* were significantly upregulated in DDC liver relative to normal liver. Chronic liver injury caused by DDC diet induces oval cells in mice, whereas PH and carbon tetrachloride-induced acute hepatitis do not. Next, the expression of the candidate genes was compared by northern blotting among normal liver, DDC liver and models of acute hepatitis, resulting in the identification of six of the nine genes that were specifically upregulated in the DDC liver, but not in the other livers (Fig. 1A). The remaining three genes, *Lyve1*, *gp130* and *Fxyd5*, were upregulated in an acute hepatitis model, suggesting that they might be involved in inflammation (data not shown). Because the expression of EpCAM, mucin 1, CD44 and

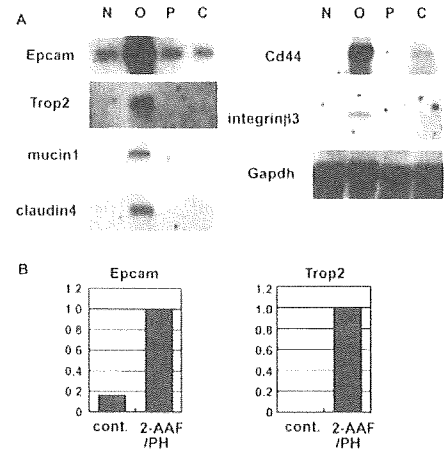

Fig. 1. Expression profiles of candidate genes in normal and injured mouse and rat liver. (**A**) Northern blot analysis of candidate genes in mouse liver. The expression of these genes was selectively upregulated in DDC liver, but not in injured liver without oval cell activation. (**B**) Quantitative RT-PCR of *Epcam* and *Trop2* in rat liver. Whereas *Epcam* was expressed in normal rat liver (cont.) and upregulated in 2-AAF/partial hepatectomy (PH)-treated liver, *Trop2* was not expressed in normal liver but was expressed in 2-AAF/PH-treated liver. N, adult mouse normal liver; O, DDC liver (6 weeks); P, liver 48 hours after 70% PH; C, liver 24 hours after carbon tetrachloride administration.

claudin 4 has been reported to be upregulated in the rat oval cell fraction (Yovchev et al., 2007), the characteristics of mouse oval cells in the DDC model appear similar to those of rat oval cells in the 2-AAF/PH model. In this study, we have focused on two structurally related type-I membrane proteins, EpCAM and TROP2. EpCAM is known to be expressed in many types of normal epithelial cell as well as in tumor cells (Armstrong and Eck, 2003; Went et al., 2004). In the liver, EpCAM is expressed on cholangiocytes but not on hepatocytes (de Boer et al., 1999; Momburg et al., 1987). Consistent with previous studies (Yovchev et al., 2007; Yovchev et al., 2008), real-time PCR showed that *Epcam* was expressed in normal rat liver and its expression was upregulated by 2-AAF/PH (Fig. 1B). As for mouse oval cells, Gleiberman et al. reported that EpCAM is expressed in oval cells upon carbon tetrachloride-induced liver injury (Gleiberman et al., 2005). However, the expression status of EpCAM in DDC liver and the nature of isolated EpCAM$^+$ cells have remained unknown. By contrast, *Trop2* was expressed in both rat and mouse injured liver, but not in normal liver (Fig. 1). TROP2 is a member of the EpCAM family and exhibits nearly 50% homology with EpCAM. TROP2 has been shown to be expressed in various tumors, whereas its expression in the liver was not known. We further examined the expression of EpCAM and TROP2 on mouse oval cells in DDC liver and investigated the nature of isolated EpCAM$^+$ cells.

Expression of EpCAM in mouse hepatic oval cells

As shown in Fig. 2A, after 4 weeks of DDC diet feeding, the mouse liver turned black because of hepatic porphyria resulting from the inhibition of the heme biosynthetic pathway (Fonia et al., 1996). Hematoxylin and Eosin (H&E) staining was performed in adult normal liver and DDC liver. The DDC liver clearly showed numerous small cells with a large nucleus around the portal veins (Fig. 2B). Immunohistochemistry (IHC) for CK19, a marker for oval cells and

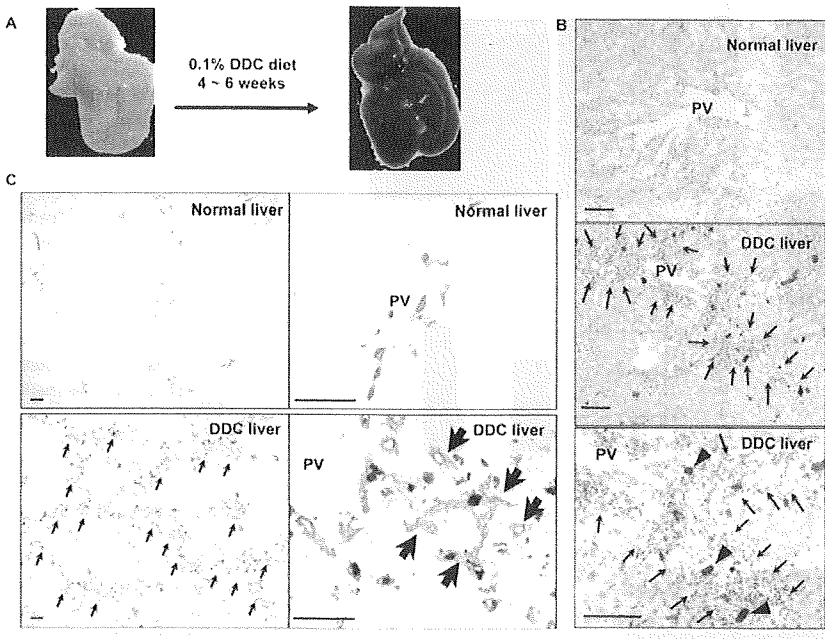

Fig. 2. DDC diet causes hepatic injury and oval cell activation. (**A**) The liver turned black after mice were fed a DDC diet. (**B**) H&E staining of a frozen section of mouse normal liver (top) and 4 weeks after DDC feeding (middle and bottom). Numerous small cells appeared around the portal veins in the DDC liver (arrows). The brown clots represent the deposition of iron hemes (arrowheads). (**C**) Immunohistochemistry (IHC) with anti-CK19 antibody showed that these numerous small cells included CK19-expressing oval cells (arrows) in DDC liver. PV, portal vein. Scale bars: 100 μm

cholangiocytes, demonstrated that these cells included oval cells as well as other CK19-negative cells, such as inflammatory cells and fibroblasts (Fig. 2C). Since EpCAM expression was upregulated in DDC liver, it was examined by IHC using sections of normal liver and of liver from mice fed DDC for 1 or 4 weeks. EpCAM$^+$ bile ducts were located adjacent to the portal vein in normal liver as reported previously (de Boer et al., 1999; Hreha et al., 1999; Joplin et al., 1990), whereas there were many EpCAM$^+$ cells forming ductular structures away from the portal vein in DDC liver (Fig. 3A). IHC with both anti-EpCAM and anti-CK19 antibodies demonstrated that all CK19$^+$ cells expressed EpCAM in DDC liver (Fig. 3B). Thus, all oval cells expressing CK19 also expressed EpCAM. To further investigate the EpCAM$^+$ cells, we generated rat monoclonal antibodies against mouse EpCAM that were applicable for flow cytometry (FCM). FCM of NPCs prepared from DDC liver showed that neither CD45 (PTPRC) nor PECAM was expressed on EpCAM$^+$ cells, indicating that EpCAM$^+$ cells are not hematopoietic or endothelial cells (Fig. 3C). Furthermore, the isolated EpCAM$^+$ cells were individually examined by immunostaining after cytospin. Almost all the sorted cells were immunostained with anti-CK19 antibody as well as A6 antibody, a mouse oval cell marker (Engelhardt et al., 1993) (Fig. 3D). Hepatic oval cells are known to be highly proliferative. To investigate their proliferation in vivo, the isolated EpCAM$^+$ cells were stained with anti-Ki67 antibody (Fig. 3E). Whereas the percentage of Ki67$^+$ cells in the isolated EpCAM$^+$ cells was ~1% in normal liver, it was 12.2% after 1 week on the DDC diet and increased to 17.4% after 4 weeks (Fig. 3F). These results strongly suggested that EpCAM is expressed in proliferating oval cells and that anti-EpCAM antibody is useful for isolating oval cells from mice fed with DDC.

TROP2 is a novel marker for mouse oval cells

Because TROP2 expression was specifically upregulated in both the mouse and rat injury models with oval cell activation (Fig. 1), TROP2 was anticipated to be expressed in oval cells. To reveal TROP2-expressing cells in normal and injured liver, we performed IHC with anti-EpCAM and anti-TROP2 antibodies. In contrast to EpCAM, TROP2 was not expressed in normal mouse liver (Fig. 4A). However, numerous TROP2$^+$ cells appeared around the portal area in DDC liver (Fig. 4B). Double immunostaining of TROP2 and EpCAM clearly showed that most of the EpCAM$^+$ cells co-expressed TROP2 in DDC liver, suggesting that TROP2 is a novel marker for oval cells (Fig. 4B). Although we could not distinguish the original bile duct in DDC liver, almost all EpCAM$^+$ cells expressed TROP2. FCM of the NPCs prepared from DDC liver also showed that the expression level of TROP2 and the population of TROP2$^+$ cells among EpCAM$^+$ cells gradually increased upon ingestion of the DDC diet (Fig. 4C). Consistent with the result of IHC, whereas TROP2 was not present in cholangiocytes expressing EpCAM at day 0, almost all EpCAM$^+$ cells became TROP2$^+$ in the DDC-fed mice and EpCAM$^+$ TROP2$^-$ cells were hardly detected after 4 weeks, suggesting that cholangiocytes themselves might also begin to express TROP2 by oval cell activation in the DDC model. Alternatively, it is also possible that TROP2$^+$ oval cells differentiate into mature cholangiocytes and replace the pre-existing cholangiocytes damaged by DDC administration.

Characterization of mouse oval cells

To reveal the characteristics of mouse oval cells, the gene expression profile of freshly isolated EpCAM$^+$ cells from DDC liver was examined by RT-PCR. As previously reported in rat oval cells, mouse EpCAM$^+$ cells also expressed both cholangiocytic markers [*Ck19*, *Ck7* (*Krt7*) and *Ggt1*] and a hepatocytic marker (*Alb*), whereas the other NPCs did not (Fig. 5A). Consistent with the previous report that AFP expression was rarely detected in mouse oval cells (Jelnes et al., 2007), AFP was not detected in mouse EpCAM$^+$ cells (data not shown). Rat oval cells were reported to express c-KIT, CD34 and THY1 (Petersen et al., 1998). It was also reported that CD133 (PROM1) is expressed in both mouse and rat oval cells (Rountree et al., 2007; Suzuki et al., 2008; Yovchev et al., 2008). Taking advantage of FCM using the anti-EpCAM antibody, we investigated the expression of these oval cell markers in EpCAM$^+$ cells before and after DDC feeding (Fig. 5B) and found